

Neuroprotective Efficacy of Saffron Aqueous Extract on Streptozotocin-Induced Rat Model of Alzheimer's Disease

Naglaa H. Eldewany

naglaahossam03@gmail.com

Alexandria University

Seham Z. Nassar

Alexandria University

Abeer Salama

National Research Centre

Sabah G. El-Banna

Alexandria University

Aly B. Okab

Alexandria University

Article

Keywords: Alzheimer's, Saffron, MBP, p-tau217, amyloid β -Peptide, Behavioural test

Posted Date: December 19th, 2025

DOI: <https://doi.org/10.21203/rs.3.rs-7957867/v1>

License:  This work is licensed under a Creative Commons Attribution 4.0 International License.

[Read Full License](#)

Additional Declarations: No competing interests reported.

1 **Neuroprotective Efficacy of Saffron Aqueous Extract on Streptozotocin-Induced Rat Model of**
2 **Alzheimer's Disease**

3 **Naglaa H. Eldewany^{a*}, Seham Z. Nassar^b, Abeer Salama^c, Sabah G. El-Banna^a, Aly B.Okab^a**

4 ^a Department of Environmental Studies, Institute of Graduate Studies and Research, Alexandria University,
5 Alexandria, Egypt. P. O:832-Postal Code: 21526; naglaahossam03@gmail.com, profokab@yahoo.com,
6 sabah_gaber@yahoo.com.

7 ^b Department of Medical Physiology, Faculty of Medicine, Alexandria University, Alexandria, Egypt.
8 drsehamn2001@yahoo.com

9 ^c Department of Pharmacology, National Research Centre, Dokki, Cairo, Egypt. P.O., 12622.
10 Berrotect@yahoo.com

11

12 **Corresponding author**

13 **Name: Naglaa H. Eldewany**

14 **Email: naglaahossam03@gmail.com**

15 **Phone Number: +0201228260193**

16

17

18

19

20

21

22

23

24

25

26

27

28

29

30

31 **Abstract**

32 Saffron is regarded as a mood enhancer. Moreover, ethnopharmacological research demonstrates that saffron
33 exhibits efficacy against neurodegenerative illnesses, specifically dementia and Parkinson's disease, due to its
34 bioactive ingredients. The purpose of this work is to assess the potential protective effect of saffron extract in
35 alleviating induced brain damage symptoms in male rats such as myelin basic protein (MBP) and serum
36 Phosphorylated tau-217 (p-Tau 217).

37 The research conducts that administration of saffron aqueous extract with the three different doses (20,40 and 80
38 mg/kg) noteworthy decrease the levels of serum phosphorylated tau-217 and in all treated groups. Myelin basic
39 protein significantly decreased in all treated groups. Additionally, there was a significant decrease in the levels
40 of inflammatory markers in the hippocampus tissue homogenate of all saffron treated groups when compared to
41 the induced group. Moreover, all saffron treated groups showed a significant decrease in levels of level of
42 gamma glutamyl transferase, acetylcholinesterase (AChE), beta-site amyloid precursor protein cleaving enzyme-
43 1 (BACE1), and amyloid β -Peptide (1-42) (A β 1-42) compared to the induced group. Supplementation with
44 saffron crude extract (SCE) significantly attenuates the formation of A β plaque and p-Tau 217 in the
45 hippocampus at different doses. In addition, SCE also counters Alzheimer -induced neuroinflammation.

46 **Keywords:** Alzheimer's, Saffron, MBP, p-tau217, amyloid β -Peptide, Behavioural test

47

48 **1. Introduction**

49 Alzheimer's disease (AD) is a prevalent neurodegenerative disorder. Currently, the precise
50 pathophysiology of Alzheimer's disease remains uncertain. However, research has indicated that the primary
51 features of AD include the deposition of β -amyloid (A β), the formation of neurofibrillary tangles, and neuronal
52 death. Hence, the dampening of neuronal apoptosis triggered by A β protein is a viable approach for the
53 prevention and management of Alzheimer's disease [1, 2].

54 The epidemiology of Alzheimer's disease is interconnected with that of all-cause dementia. While
55 Alzheimer's disease is the predominant etiology of dementia, many neurodegenerative or cerebrovascular
56 disorders can also precipitate dementia, especially in elderly individuals. In a study involving 184 individuals
57 who satisfied the neuropathological criteria for Alzheimer's Disease (AD), 31% exhibited solely AD pathology,
58 22% presented with AD pathology alongside α -synuclein pathology, 29.5% had AD pathology in conjunction
59 with TDP-43 pathology, and 17.5% displayed both α -synuclein and TDP-43 pathology alongside AD pathology.
60 In each of these pathologically defined categories, 29% to 52% of patients exhibited at least one infarct
61 (microinfarct, lacunar infarct, or big infarct) [3].

62 Streptozotocin (STZ), or 2-deoxy-2-(3-(methyl-3-nitrosoureido)-D-glucopyranose), is a naturally
63 occurring antibiotic synthesized by Streptomyces achromogenes derived from glucosamine nitrosourea. The
64 primary model for sporadic Alzheimer's disease in rats is based on the effects of STZ, which aligns with the
65 sporadic variety in humans. Additionally, STZ induces neuronal injury and hyperphosphorylation of tau, leading
66 to the production of reactive oxygen species (ROS) and reactive nitrogen species [4].

67 The accumulation of A β is a defining pathogenic hallmark in both well-studied autosomal dominant
68 Alzheimer's disease and sporadic late-onset Alzheimer's disease patients. A β is produced through the processing
69 of APP, a transmembrane glycoprotein, by sequential cleavage by γ -secretase and β -secretase, a multiprotein
70 complex that includes PS1 or PS2 as catalytic subunits [5].

71 Myelin basic protein (MBP), the second most abundant protein in the central nervous system, is
72 responsible for adhesion of cytosolic surfaces of multilayered compact myelin. It interacts with polyanionic
73 proteins and negatively charged lipids, potentially acting as a membrane actin-binding protein. MBP may also
74 participate in signalling; oligodendrocytes and myelin use it for different purposes [6].

75 An accurate blood test for Alzheimer's disease would significantly impact the process of selecting
76 participants for clinical trials. It would enable the pre-screening of non-demented individuals in a way that is
77 minimally invasive and cost-effective. This would reduce the need for additional testing using more invasive and
78 expensive methods such as CSF analyses or PET scans [7].

79 Phosphorylated tau (p-Tau) is now the most promising candidate for new blood tests for Alzheimer's
80 disease (AD), showing superior precision in diagnosis and specificity for the disease compared to other
81 suggested blood biomarkers [8]. Out of the suggested blood p-Tau biomarkers [9], phosphorylated tau at
82 Threonine 217 (p-Tau217) has consistently demonstrated excellent performance in distinguishing Alzheimer's
83 disease (AD) from other neurodegenerative disorders and in identifying AD pathology in patients with mild
84 cognitive impairment. It is worth mentioning that p-Tau217 shows more significant differences in comparison to
85 p-Tau181 and p-Tau231, often achieving high levels of distinction. Moreover, p-Tau217 has a distinct pattern of
86 change over time in individuals with amyloid, with notable increases that are strongly linked to the progression
87 of cortical atrophy [10].

88 The scientific community is currently confronted with the formidable task of identifying dependable
89 natural substances that provide practical potential for the treatment of neurological illnesses, such as Alzheimer's
90 disease [11].

91 Saffron, commonly known as 'Kesar' belongs to the dried stigma of *Crocus sativus* L., family Iridaceae,
92 used as one of the dietary supplements worldwide. It has footprints in many traditional scriptures for its
93 medicinal purposes. In India, saffron mainly grows in Kashmir and is known as Kashmir or Indian Saffron. [12].

94 Considering their acceptable efficacy and a more favourable safety profile, herbal remedies have attracted
95 more attention as novel promising entities for improving or at least decreasing cognitive deterioration in patients
96 with AD. Effectiveness of herbal compounds in counteracting different central nervous system-affecting
97 disorders and cognitive deficits has been determined in numerous experimental and clinical research. Saffron is
98 the dried stigma of a plant named *Crocus sativus* L. and has been known as the world's most expensive spice and
99 a widely used medicinal plant. From a chemical standpoint, the main constituents of saffron are carotenoids

100 (crocin), esters (crocetin), and aldehydes (picrocrocin and safranal). In the recent decades, a growing body of
101 evidence has revealed encouraging beneficial effects for saffron in treating different neuropsychiatric disorders
102 such as depression, seizure, anxiety, and memory disorders. Similarly, promising advantages of saffron in
103 improving different cognitive functions have been demonstrated in multiple preclinical studies. Saffron
104 administration in animals can reverse memory deficits in different behavioural tasks, exerts protective effects
105 against neuronal injury, and positively affects learning behaviour, recognition, spatial memory, and long-term
106 potentiation [13].

107 A handful of studies have been undertaken to assess the impact of standardised SCE on the dysregulated
108 cholinergic system and associated biochemical and histological alterations in the brain. The present study
109 examined the mitigating effects of standardised SCE supplementation on cognitive impairment and biochemical
110 and immunohistochemical alterations, such as the formation of A β plaques and p-Tau 217, generated by
111 Alzheimer's disease induction by (STZ) by 3mg/kg. The study emphasises the significance of SCE
112 phytoconstituents in modulating the dysregulated cholinergic system for use as herbal nutraceuticals.

113 **2. Material and Methods**

114 **2.1. Sample preparation for high-performance liquid chromatography (HPLC)**

115 To determine the way of extraction of saffron to obtain the higher concentration of saffron components,
116 ethanolic and water extracts were prepared in the same way: 10 mL of ethanol and 10 mL of water were added to
117 1 g of intact stigmata of saffron and macerated for about 3 days in the dark at ambient temperature with
118 occasional stirring [14]. The crude ethanolic and water extract was analysed by HPLC.

119 **2.1.1. HPLC conditions**

120 Analysis by HPLC was conducted using an Agilent 1260 series. The separation was conducted using a
121 Zorbax Eclipse Plus C8 column (4.6 mm x 250 mm i.d., 5 μ m). The mobile phase consisted of water (A) and
122 0.05% trifluoroacetic acid in acetonitrile (B) at a flow rate of 0.9 mL/min. The mobile phase was programmed
123 consecutively in a linear gradient as follows: 0 min (82% A); 0–1 min (82% A); 1–11 min (75% A); 11–18 min
124 (60% A); 18–22 min (82% A); 22–24 min (82% A). The multi-wavelength detector was monitored at 280 nm.
125 The injection volume was 5 μ L for each of the sample solutions. The column temperature was maintained at
126 40°C.

127 **2.1.2. Preparation of saffron crude aqueous extract**

128 Saffron (*Crocus sativus L.*) was collected from Estahban, 170 km east of Shiraz, Iran, on 20 January 2024. The
129 plant was identified by **Soliman M. Toto**, Associate Professor of Plant Ecology, Department of Botany and
130 Microbiology, Faculty of Science, Alexandria University. A voucher specimen was deposited at the Herbarium of
131 Alexandria University, no. ALEX 4125. The stigma was immersed in distilled water for a duration of 3 days at a
132 temperature of 4°C, without exposure to light, and with constant agitation. The extract underwent filtration using
133 gauze to get a clear extract.

134 **2.2. Total antioxidant capacity**

135 Several assays were developed for the assessment of the total antioxidant capacity of compounds and
136 herbal extracts. The chemical bases of these assays differ significantly, and the results obtained are associated
137 with specific chemical properties of the screened compounds rather than their biological antioxidant capacity
138 [15].

139 **2.2.1. Azino-bis-3-ethylbenzothiazoline-6-suLphonic acid (ABTS) assay**

140 The assay was carried out according to the method of adopting the modifications of Re et al. (1999) [16]:
141 Briefly, the study involved dissolving 192 mg of ABTS in distilled water, adding it to 140 mM potassium
142 persulphate, and then adding methanol to obtain the final ABTS dilution. The reagent was mixed with 10 μ L of
143 the sample/compound in a 96-well plate, and the colour intensity was measured at 734 nm. At the end of the
144 incubation time, the decrease in ABTS's colour intensity was measured at 734 nm. Data are represented as means
145 \pm SD according to the following equation:

$$146 \text{Percentage inhibition} = \left(\frac{\text{Average absorbance of blank} - \text{average absorbance of the test}}{\text{Average absorbance of blank test}} \right) * 100$$

147

148 **2.2.2. Oxygen radical absorbance capacity assay (ORAC)**

149 The assay was carried out according to the method of Ou et al., (2002) [17].

150 **2.2.3. Acetylcholinesterase inhibition assay**

151 The assay was carried out according to the method of Vinutha et al., (2007) [18] with minor
152 modifications. Briefly, 10 μ L of the indicator solution (0.4 mM in buffer (1): 100 mM Tris buffer pH 7.5) was
153 transferred to a 96-well plate, followed by 20 μ L of enzyme solution (acetylcholine esterase 0.02 U/mL final
154 concentration in buffer (2): 50 mM Tris buffer pH 7.5 containing 0.1% bovine serum albumin). Next, 20 μ L of
155 the sample/standard solution was added, followed by 140 μ L of buffer (1), and this step was repeated with
156 another 20 μ L of the sample/standard solution and an additional 140 μ L of buffer (1). The mixture was allowed
157 to stand for 15 min at room temperature. Afterwards, 10 μ L of the substrate (0.4 mM acetylcholine iodide
158 buffer) was added immediately to all wells. The plate was incubated in a dark chamber for 20 minutes at room
159 temperature. At the end of the incubation period, the colour was measured at 412 nm. Data are represented as
160 means \pm SD.

161 **2.3. Experimental Animals**

162 Forty healthy male albino rats (*Rattus norvegicus*), each averaging 210 \pm 10 g and two months old, were
163 obtained from the animal house at the Faculty of Medicine, Alexandria University, and acclimated for two weeks
164 before the experiment. They were assigned to 8 groups and housed in Universal galvanized wire cages at room
165 temperature (22-25°C) and in a photoperiod of 12/12 h/day. Animals were provided with a balanced commercial
166 diet containing 18% crude protein, 14% crude fiber, 2% fat, and 2600 Kcal DE/kg feed.

167 **2.4. Ethics statement**

168 The experiments were approved by the Ethical Committee of the National Research Centre, Egypt, and the
169 Institutional Animal Care and Use Committee, Faculty of Medicine, Alexandria University (ALEXU-IACUC
170 No. AU14-231130-2-12), Alexandria, Egypt. All experiments with animals complied with the ARRIVE (Animal
171 Research:Reporting of In Vivo Experiments) guidelines (<https://arriveguidelines.org>).

172 **2.5. Experimental Design**

173 Animals were randomly divided into 8 equal groups and assigned as follows:

174 The sham group received a citrate buffer via intracerebroventricular (ICV) injection, while the induced
175 group was injected once with 3 mg/kg body weight of streptozotocin (STZ) using citrate buffer as a vehicle.
176 After 30 days of intracerebral ventricular (ICV) STZ injection, animals' neurodegenerative alterations induced by
177 ICV-STZ were evaluated [19], Saffron crude extract was administered for one month daily orally through
178 gavage in three different doses: 20 mg/kg (SD20), 40 mg/kg (SD40), and 80 mg/kg (SD80) [20]. The remaining
179 three groups were induced with STZ and after that administered with different doses of saffron extract (ISD20,
180 ISD40, and ISD80, respectively).All experiments and treat with animals where according to the Animal Care
181 Guidelines and accept responsibility for the conduct of the experimental procedures detailed in this proposal in
182 accordance with the guidelines contained in the Guide for the Care and Use of Laboratory Animals 8th Edition
183 2011

184 **2.6. Induction of experimental dementia of AD in male rats**

185 The animals were initially administered intraperitoneal (i.p.) injections of ketamine (100 mg/kg) and
186 xylazine (10 mg/kg) to induce anesthesia. Streptozotocin was administered unilaterally into the lateral ventricle
187 using a Hamilton syringe, with a dosage of 3 mg/kg, 4 μ l per injection site, using stereotaxic surgery [21].
188 According to BÜTner-Ennever, (1997) [22] the ICV injection was performed using the following coordinates:
189 0.8 mm posterior to the bregma, 1.5 mm lateral to the sagittal suture, and 3.6 mm ventral from the surface of the
190 brain. The meninges were meticulously preserved without any injury throughout the surgery. The injection of a 3
191 mg/kg STZ solution was performed using a Hamilton syringe with a cannula diameter of 0.3 mm. Shortly prior
192 to administration, STZ was dissolved in a citrate buffer (0.05M, pH:4.5) and subsequently injected unilaterally
193 into the ventricle of the brain. After the injection, the cannula was left in place for an additional 5 min to
194 facilitate passive diffusion from the tip of the cannula and reduce the distribution of the substance throughout the
195 injection tract. Subsequently, the cannula was gradually extracted from the scalp and secured using sutures.
196

197 **2.7. Behavioral tests**

198 **2.7.1. Morris water maze**

199 To assess the rats' spatial learning and memory, the Morris Water Maze (MWM) was conducted over the
200 final seven days of the experiment. The maze consists of a grey circular metal tank (180 cm in diameter) that is
201 filled with water at a temperature of approximately $22 \pm 3^{\circ}\text{C}$. The water depth is 30 cm. The water was rendered
202 opaque by adding non-toxic paint. The pool was partitioned into four quadrants, each delineated by distinct
203 beginning locations on its wall: north, south, east, and west (N–S–E–W). Inside the tank, there is a circular black
204 platform with a diameter of 10 cm. This platform is located in the SW quadrant 20 cm away from the tank's edge
205 and is submerged 1 cm below the water's surface. Extra maze cues were placed around the tank in the room.
206 Each of the experimental rats underwent daily water maze training consisting of four trials per day from different
207 start locations for a duration of six days. Memory recall testing was conducted 24 h following the sixth day,
208 during which the platform was taken away and each rat was given 60 s of unrestricted swimming. The
209 percentage of time is determined by dividing the time spent in the target quadrant by the total time and then
210 multiplying the result by 100. Similarly, the percentage of distance is calculated by dividing the distance swum
211 in the target quadrant by the total distance swum and then multiplying the result by 100 [23, 24].

212 **2.7.2. Novel object recognition (NOR) task**

213 The object recognition task, a behavioural test, was conducted in the last two days of the treatment period.
214 The test assumes that animals explore the novel object as their natural propensity to the novelty and that novel
215 stimuli can change animals' behaviour, provoke stress responses, and elicit approach behaviour. The
216 experimental setup consisted of open-field boxes with dimensions of $20 \times 20 \times 17$, which were sparsely lighted.
217 Initially, habituation was conducted by placing each rat individually in one of the boxes for a duration of 15 min.
218 The subsequent day, the familiarisation phase was done by placing a pair of plastic sample objects, positioned
219 roughly 12 inches apart, inside one of the boxes. The rats were then given a 10-min period to explore the objects.
220 Following a 3-h interval, the rats had a retention test in which they were placed back in the open field. However,
221 one of the objects from the training session was replaced with a new object of similar size and complexity. The
222 rats were allowed to explore for 5 min; the total time spent exploring each of the two objects (when the animal's
223 snout was directly towards the object at a distance ≤ 2 cm) was recorded. The recognition index (RI) was
224 employed to quantify memory recognition in the study. RI refers to the percentage of time spent investigating
225 either the familiar object or the novel item out of the total time spent exploring both objects. This calculation is
226 derived from the formula $\text{RI} = (\text{time spent exploring familiar object or novel object} / \text{total time spent exploring}$
227 both objects) $\times 100$ [25].

228 **2.8. Biochemical analysis**

229 **2.8.1. Determination of phosphorylated tau-217 (p-Tau 217) blood-based biomarker**

230 At the end of treatment period in the last week behavioral tests were performed then rats were
231 anesthetized using anhal consist of isoflurane 100% (Anesthetic liquid for inhalation), after that rats were
232 weighed before scarification. Minimal pain and distress are anticipated as the animals will be well-fed, cared for,
233 and anesthetized before the sacrifice. Then they were desiccated, blood was collected from the heart, in Serum
234 Separator tubes to obtain blood serum. Blood was collected in a serum separator tube and then centrifuged at
235 1000 xg for 15 min. The obtained serum was used to estimate the activities of phosphorylated tau-217 (p-Tau
236 217), which were determined using ELISA kits procured from Shanghai Ideal Medical Technology Co., Ltd.

237 **2.8.2. Determination of gamma-glutamyl transferase (GGT) and butyryl cholinesterase (BChE) activity**

238 Gamma-glutamyl transferase (GGT; EC 2.3.2.2) and butyryl cholinesterase (BChE; EC: 3.1.1.8) were
239 measured according to the methods of [26], respectively. The kits were obtained from **Bio Diagnostic**, Egypt.

240 **2.9. Preparation of brain hippocampus homogenate**

241 The rats were sacrificed by decapitation. The brains were scooped out, rinsed with normal saline, and the
242 hippocampi were identified and dissected out for demolition in a tissue homogenization using a tissue
243 homogenizer (HG-15D) using 0.01 M phosphate buffer (pH 7.4). The tissue-buffer ratio was 1:9 buffer by
244 weight/volume. Centrifugation of homogenates was conducted at 10000 xg. Supernatants were collected in
245 separate aliquots and stored at -80°C for biochemical analysis.

246 **2.9.1. Estimation of myelin basic protein and acetylcholinesterase in hippocampus homogenate**

247 Myelin Basic Protein (MBP) and Acetylcholinesterase (AChE) levels were on admission in hippocampus
248 homogenate using Enzyme Linked Immunosorbent Assay (ELISA) following the production instructions
249 provided by Sunlong Biotec.

250 **2.9.2. Evaluation of beta-site amyloid precursor protein cleaving enzyme-1 and amyloid β -Peptide (1-42)**

251 The level of beta-site amyloid precursor protein cleaving enzyme-1 (BACE1) and amyloid β -peptide (1-
252 42) (A β 1-42) was determined using the respective commercial ELISA kit from Sun Red Co. LTD, Shanghai,
253 China. The kit uses a double-antibody sandwich enzyme-linked immunosorbent assay (ELISA) to assay the level
254 of rat β -site APP-cleaving enzyme 1 (BACE1) in samples. Add β -site APP-Cleaving Enzyme 1 (BACE1) to the
255 monoclonal antibody enzyme well, which is pre-coated with Rat β -site APP-Cleaving Enzyme 1 (BACE1)
256 monoclonal antibody, and incubate; then, add the (BACE1) antibody labelled with biotin and combined with
257 Streptavidin-HRP to form an immune complex; then, carry out incubation and washing again to remove the
258 unbound enzyme. Then add Chromogen Solutions A and B; the colour of the liquid changes into blue, and under
259 the effect of acid, the colour finally becomes yellow. The chroma of colour and the concentration of the Rat
260 Substance β -site APP-Cleaving Enzyme 1 (BACE1) of the sample were positively correlated. The same
261 procedure was followed to assay the level of amyloid β -peptide (1-42) in homogenate.

262 **2.9.3. Determination of inflammatory and oxidative stress biomarkers**

263 Hippocampus content of tumour necrosis factor-alpha (TNF- α), interleukin 6 (IL-6), cyclooxygenase 2
264 (COX-2), and cysteine-aspartic acid protease (Caspase-3) as an apoptotic marker were estimated using ELISA
265 kits according to the manufacturing instructions of Sunlong Biotec Co. LTD, Zhejiang, China.

266 **2.9.4. DNA breakages assay with diphenylamine reaction in hippocampus homogenate**

267 The diphenylamine DNA fragmentation percentage assay is a highly effective approach for evaluating
268 apoptosis because it determines the proportion of DNA fragmentation into oligosomal-sized particles. The
269 amount of soluble DNA released by apoptotic nuclei into the cytoplasm is a quantitative indicator of cellular
270 response. Another feature of the diphenylamine assay is that it may detect apoptotic DNA fragmentation in both
271 adhering and floating cells after treatment with chemotherapeutic or other drugs. The DNA fragmentation
272 percentage assay was performed using the procedure of Wu et al. (2006) [27].

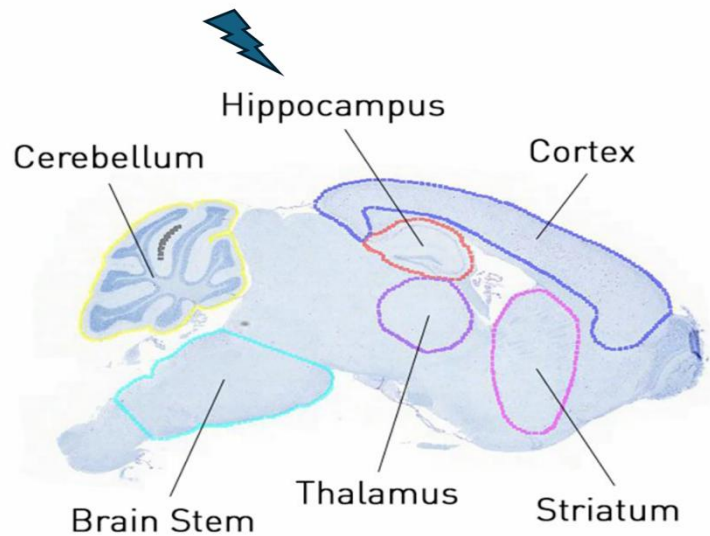
273
$$\text{Fragmented DNA (\%)} = T \times 100 / (T + B)$$

274 T: Measure absorbance of Supernatant

275 B: Measure absorbance of Pellet

276 **2.10. Immunohistochemical Examination of Amyloid β (A β) peptide plaques and tubulin-associated unit
277 (Tau)**

278 For determination of Amyloid β (A β) peptide plaques and tubulin-associated unit (Tau) in hippocampus
279 brain tissue, the tissue analysis staining technique comprises multiple phases. The slides are initially immersed in
280 a peroxidase blocking solution for 10 minutes, followed by rinsing with wash buffer to eliminate surplus liquid.
281 Subsequently, serum blocking is applied to each tissue segment and incubated for 10 minutes. The primary
282 antibody is produced, incubated for 30 to 60 minutes, and subsequently washed three times. A biotinylated goat
283 secondary antibody is applied, incubated for 10 minutes, and subsequently washed three times. An enzyme
284 conjugate is introduced, incubated for 10 minutes, and subsequently washed three times. Incubation with
285 substrate/chromogen is conducted, followed by counterstaining with Hematoxylin. Mounting and covering slips
286 are subsequently placed using Acu-stainTM Mouse + Rabbit HRP kits (Genemed Biotechnologies, inc, USA)
287 with Catalog No. 52-0003 and 54-0003. (Figure 1) [28].



288

289 **Figure (1):** Sagittal mouse brain section with ground truth test image AI segmentation

290

291 **2.11. Statistical analysis**

292 The data was presented as the mean values together with the standard error of the mean (SEM). An
293 ANOVA was conducted followed by Tukey's post hoc tests to evaluate group differences. The data was analyzed
294 using SPSS version 25. P-values below 0.05 were deemed statistically significant [29].
295

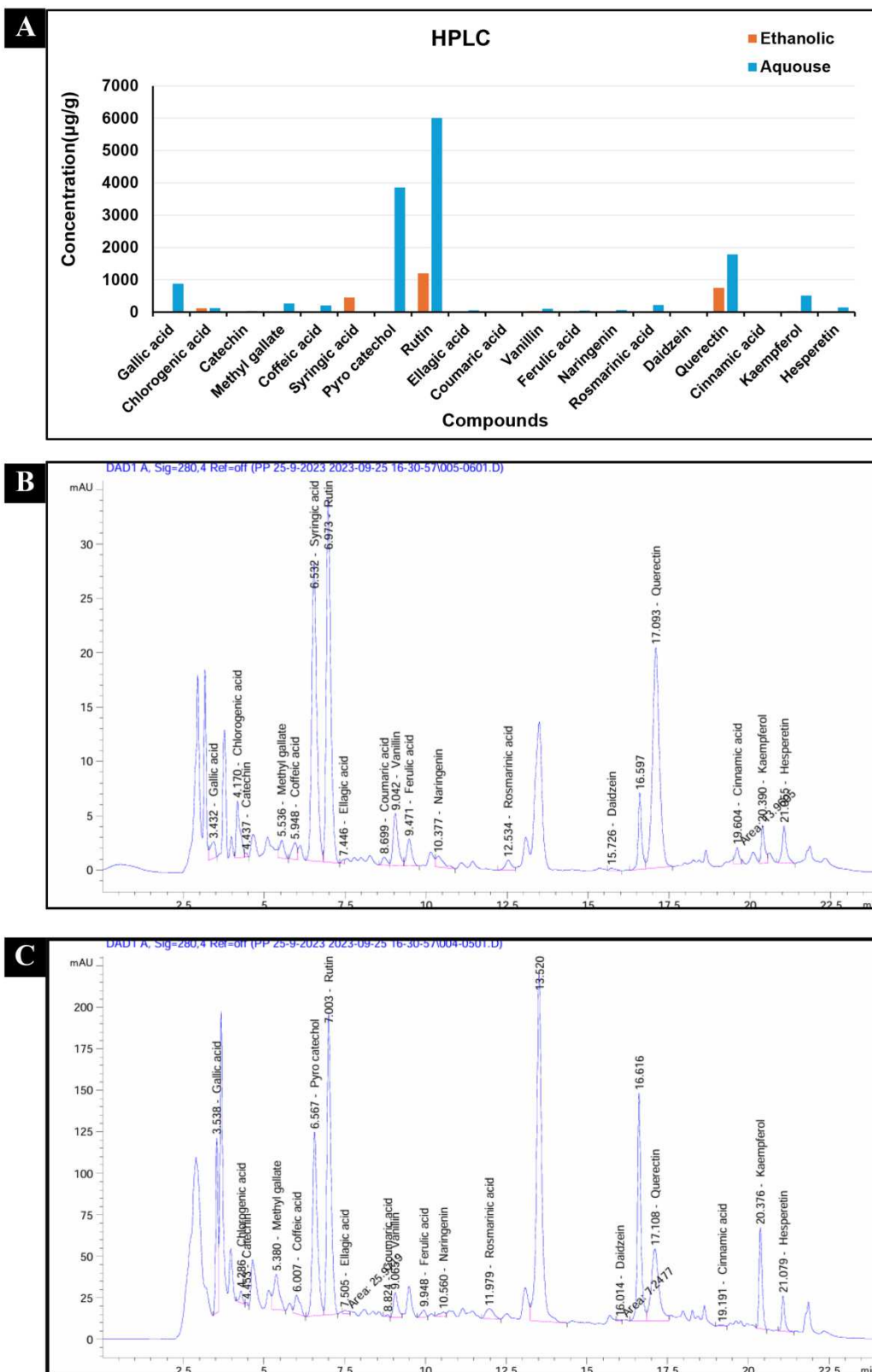
296 **3. Results**297 **3.1. Phytochemical composition of saffron extracts**

298 The chromatographic conditions used permitted the identification of key components in each sample,
 299 resulting in a unique baseline separation. **Table 1** and **Figure 2** demonstrate the results of an aqueous extract and
 300 an ethanolic extract of saffron. According to our findings, different extracts appeared to have similar chemical
 301 compositions but varying concentrations of each component.

302 **Table (1): High-performance liquid chromatography of the phytochemical composition of aqueous and**
 303 **ethanolic saffron extracts**

Extract	Ethanolic Extract ($\mu\text{g/g}$)	Aqueous Extract ($\mu\text{g/g}$)
Components		
Gallic acid	29.88	879.58
Chlorogenic acid	115.02	124.48
Catechin	8.24	35.63
Methyl gallate	16.85	266.09
Coffeic acid	26.31	207.46
Syringic acid	452.94	0.00
Pyro catechol	0.00	3854.72
Rutin	1202.03	6012.25
Ellagic acid	4.31	53.01
Coumaric acid	5.46	5.36
Vanillin	38.79	107.04
Ferulic acid	30.87	47.44
Naringenin	30.06	61.23
Rosmarinic acid	28.19	217.21
Daidzein	3.63	8.28
Quercetin	751.44	1783.85
Cinnamic acid	5.04	2.24
Kaempferol	32.89	509.82
Hesperetin	30.67	146.91

304



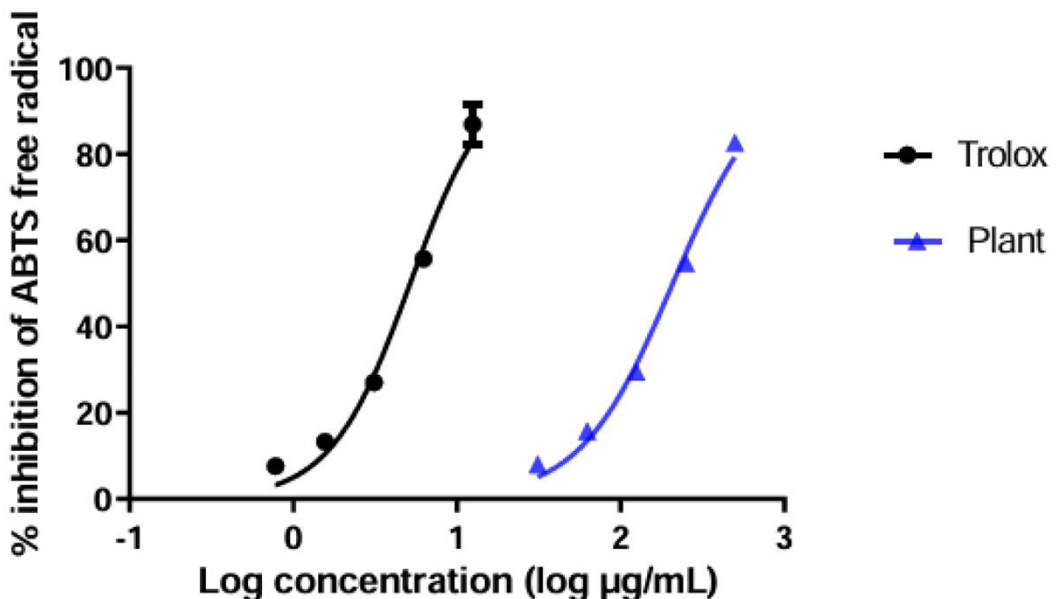
305

306 **Figure (2): (A, B and C) Chromatograms of water and ethanolic saffron extract obtained**
 307 **using high-performance liquid chromatography (A): Comparison between**
 308 **saffron water and ethanolic extract, (B): HPLC chromatogram analysis of**
 309 **saffron ethanolic extract and (C): HPLC chromatogram analysis of saffron water**
 310 **extract.**

311

312 **3.2. The ABTS radical scavenging assay**

313 The ABTS radical scavenging assay is among the most widely employed antioxidant evaluations for plant
 314 specimens. Antioxidants utilized in food are chemical substances that can donate hydrogen radicals, hence
 315 reducing rancidity and lipid peroxidation in food items. They prolong the shelf life of lipid-rich food without
 316 compromising sensory or nutritional integrity [30]. **Figure (3)** indicate that the IC₅₀ of saffron extract is 208.5
 317 $\mu\text{g/mL}$. The percentage inhibition of saffron extract at several concentrations (31.25, 62.5, 125, 250, 500 $\mu\text{g/mL}$)
 318 in aqueous extract is (7.47%, 16.76%, 29.42%, 54.19%, 81.06%).



319

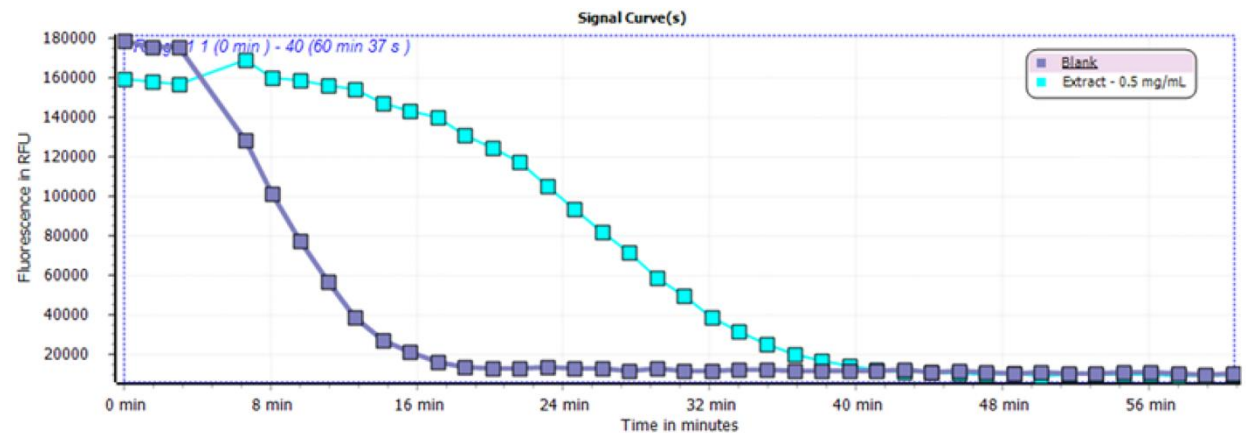
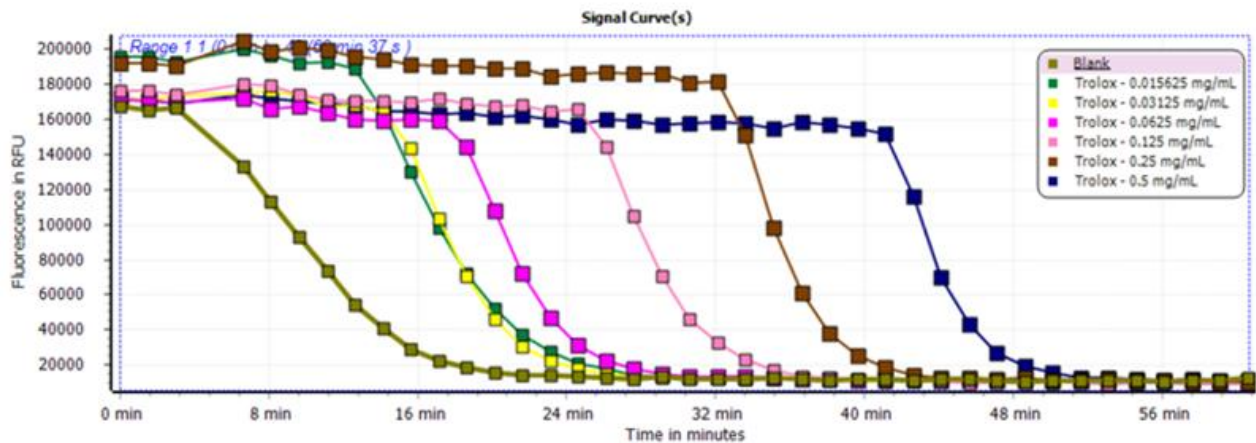
320 **Figure (3): ABTS inhibitory concentration (IC50)**321 **3.3. Oxygen radical absorbance capacity (ORAC) assay**

322 The ORAC assay evaluates an antioxidant's effectiveness by analysing the area under the curve of fluorescence
 323 intensity over time, allowing for the assessment of peroxy radical reactions with a specific compound and the
 324 determination of the total antioxidant capacity of a food extract [31]. The experiment quantifies the temporal
 325 degradation of fluorescence of fluorescein in the presence and absence of antioxidant substances. Antioxidant
 326 activity using ORAC assay is 1 μg Trolox equivalent (TE) /186.18 mg sample as observed in **Table (2)** and
 327 **Figures (4 and 5)**.

328 **Table (2): Saffron extract effect on oxygen radical absorbance capacity assay**

Sample I.D.	Av RFU	Substitution in equation 1 ($\mu\text{g/mL}$)	Antioxidant activity using ORAC assay is ($\mu\text{g TE /mg sample}$)	Standard Deviation
Saffron extract	1341887	93.09	186.18	18.10

329



338 **3.4. Acetylcholinesterase inhibitor assay**

339 Inhibition of Acetylcholinesterase (AChE), the fundamental enzyme responsible for the degradation of
 340 Acetylcholine, is seen as a potential approach for the treatment of neurological illnesses including Alzheimer's
 341 disease, senile dementia, ataxia, and myasthenia gravis. A significant supply of AChE inhibitors is undoubtedly
 342 offered by the prevalence of plants in nature [32]. The percentage inhibition of saffron extract in a dose
 343 dependant manner as the concentration increase the inhibition increase in 50 and 500 $\mu\text{g/mL}$ the percentage
 344 inhibition equal 1.41 % and 4.84 % as observed in **Table (3)**.

345 **Table (3): Acetylcholinesterase percentage inhibition of saffron extract**

Sample ID	Mean at 50 $\mu\text{g/mL}$	SD	Mean at 500 $\mu\text{g/mL}$	SD
Extract	1.41	0.21	4.84	0.67
Donepezil ($\mu\text{g/mL}$)	0.0005 $\mu\text{g/mL}$		0.5 $\mu\text{g/mL}$	
	4.61	0.31	96.20	0.24

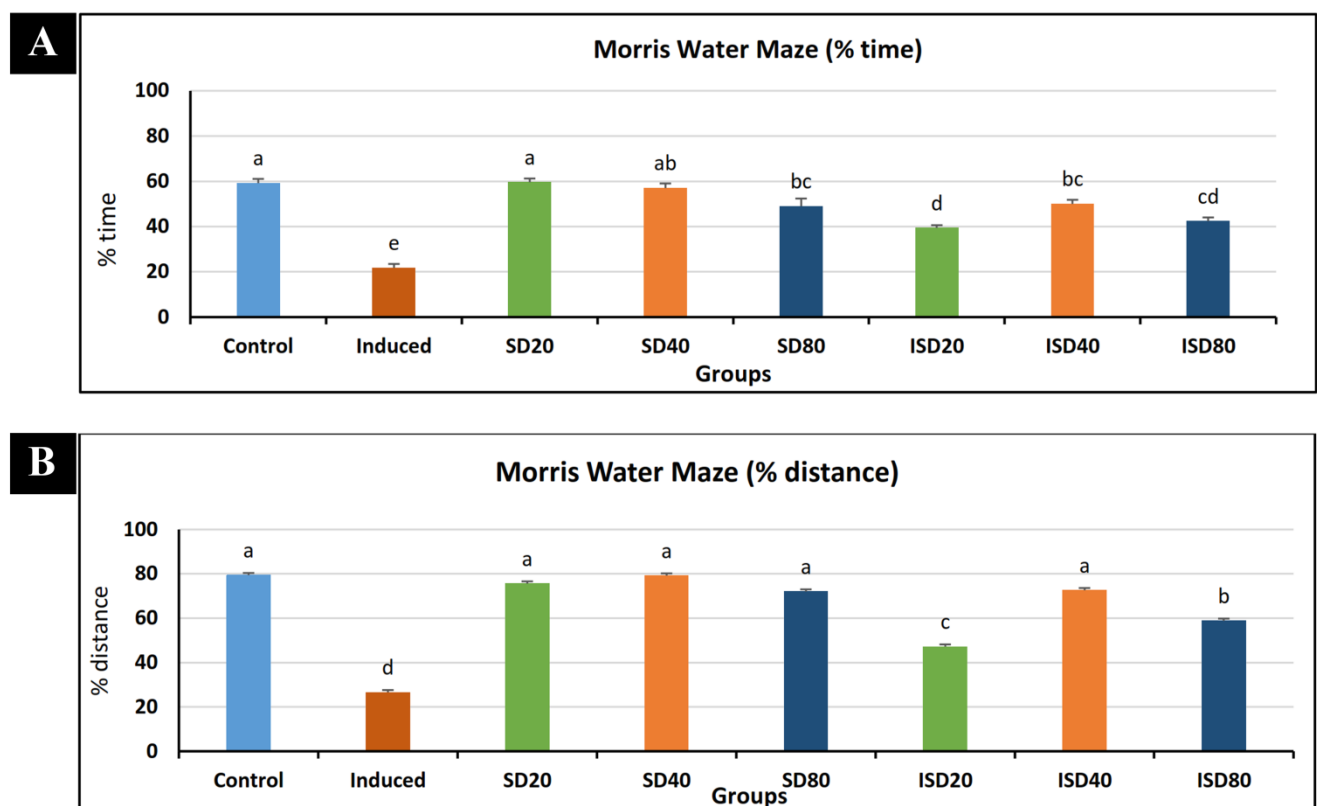
346

347 **3.5. Memory tests**

348 Administration of saffron crude extract enhances cognitive abilities related to learning and memory.

349 **3.5.1. Morris water maze**

350 **Figure 6 (a, b)** illustrates the results of the spatial memory retention test, the healthy control rats spent the
351 longest on average time and swam in the target quadrant, which suggests that memory consolidation functioned
352 effectively in this group. However, the STZ group exhibited considerably reduced time spent and swimming
353 distance in the target quadrant compared to the control group. However, treatment with various dosages of
354 saffron crude extract resulted in a considerable increase in the percentage of time spent in the intended quadrant.
355 This increase was found to be modest when compared to healthy control rats, but significantly greater than
356 untreated rats with STZ-induced AD.



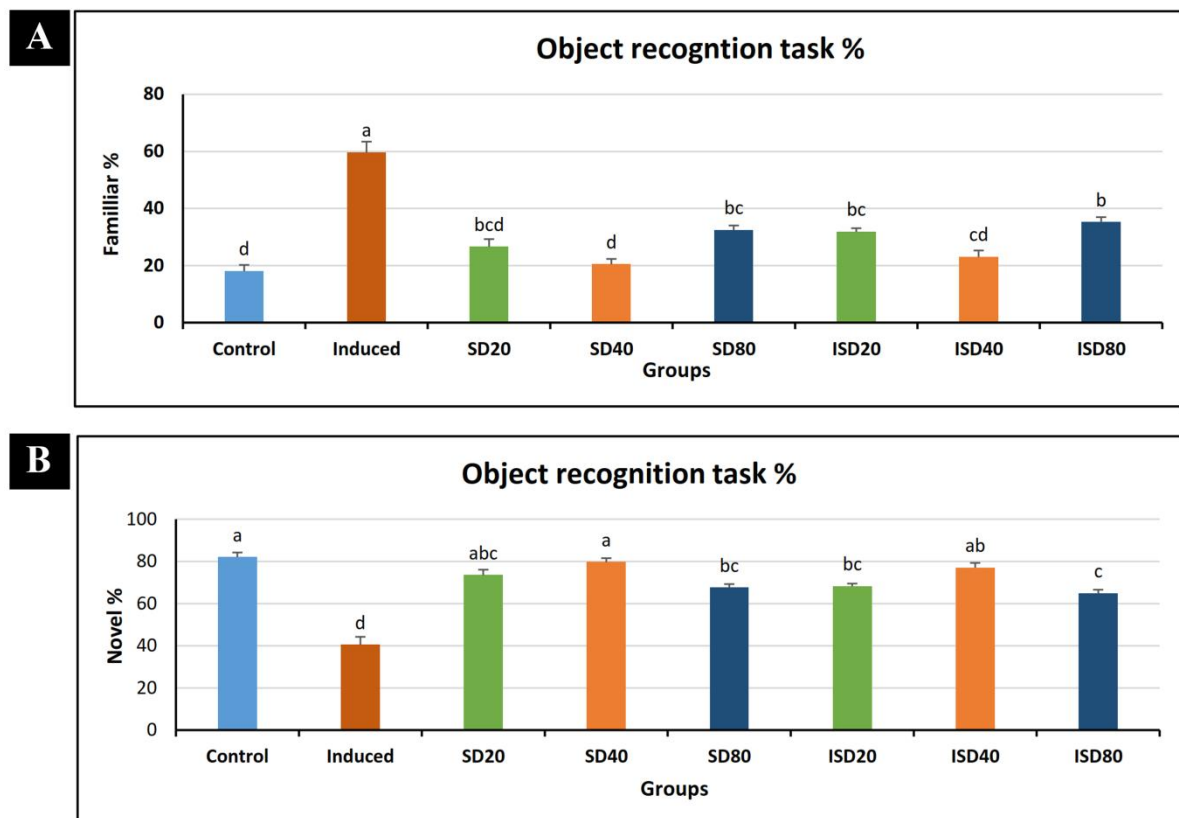
357

358 **Figure 6:** Effect of treatment on learning and memory, (A) The mean percent of time
359 spent in the target quadrant in memory retention test, (B) The mean percentage
360 of distance swum the target quadrant.

361

362 **3.5.2. Influences of saffron extract on the memory of recognizing objects**

363 Over the last week, recognition memory was assessed using the object recognition task. Typically, rats
364 exhibit a greater inclination to investigate a new object compared to a familiar one. As shown in **Figure 7 (a, b)**
365 The object recognition memory of STZ untreated rats was notably impaired, as they spent less time investigating
366 the novel objects compared to the known ones. In contrast, rats treated with SCE did not show any difference in
367 interval of time they spent with the novel and familiar objects. Nevertheless, administration of saffron crude
368 extract (20,40&80 mg/kg) to AD rats resulted in a substantial increase in the duration of exploration of the novel
369 object by (68.8%, 90.59%&60.4%) respectively, which was statistically significant compared to the induced
370 group.
371

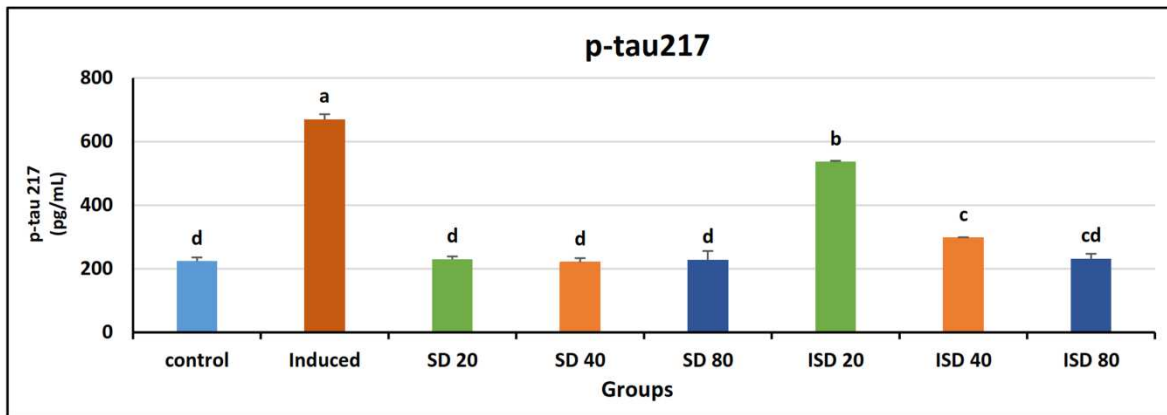


372

373 **Figure 7:** Effect of treatment on object recognition task, (A) the percent of time spent in the
 374 exploring the familiar object, (B) the percent of time spent in exploring the
 375 novel object.

376 **3.6. Saffron extract impacts on serum level of phosphorylated tau 217**

377 Levels of p-tau 217 show a considerable rise in the induced group compared to the sham group. Indeed,
 378 p-tau 217 was substantially diminished in all treated groups (20,40&80 mg/kg) compared to the induced groups
 379 by (19.9%,55.55%&65.43%) respectively as shown in **Figure 8** in addition in saffron 80 mg/kg returned p-tau
 380 217 to their level to its normal range.



381

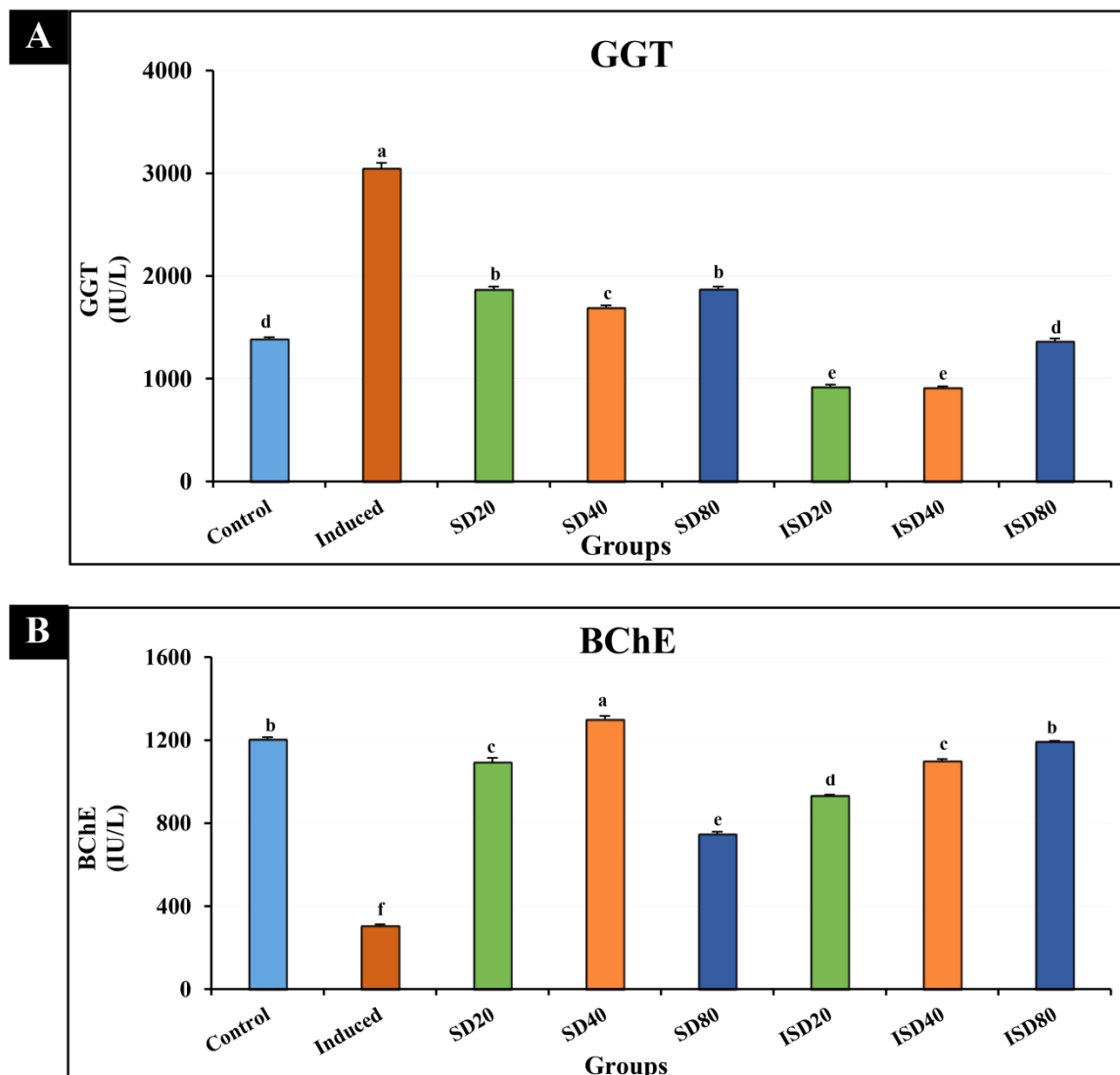
382 **Figure 8:** Phosphorylated tau 217 level in hippocampus tissue homogenate.

383

384 **3.7. Gamma-glutamyl transferase (GGT) and butyryl cholinesterase (BChE) activity in blood serum**

385 The results in **Figure 9 (a and b)** indicated that level of gamma glutamyl transferase (GGT) markedly
 386 elevated in the induced group compared to the control group. The injection of saffron crude extract significantly
 387 reduced GGT in all treated groups by (69.82%,70.11%&55.22%).

388 The findings demonstrate that serum butyrylcholinesterase (BChE) significantly diminished in the
 389 induced group compared to the control group. The injection of saffron aqueous at varying doses (**20, 40, and 80**
 390 mg/kg) considerably elevated BchE by (205.14%,259.88%&290.51%), which subsequently normalized in
 391 comparison to the stimulated group. Returning them to the normal range compared to the induced group.

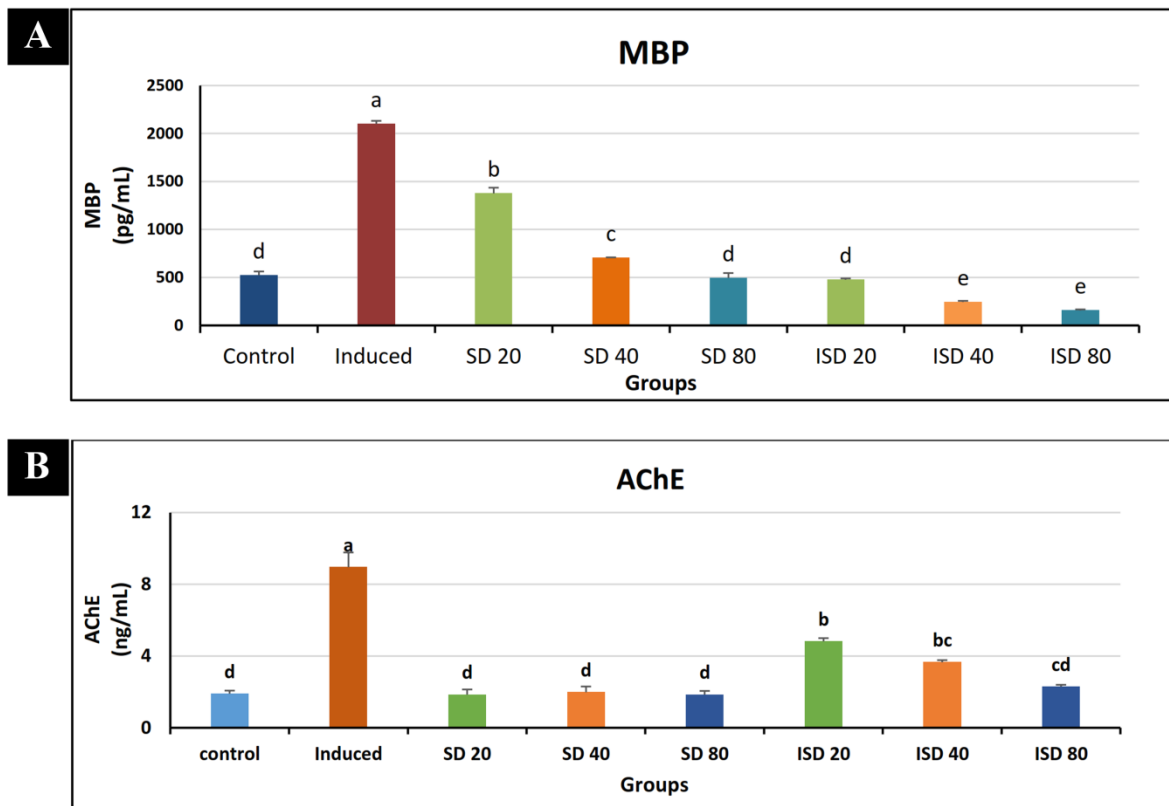


392

393 **Figure 9: (A and B) Saffron crude aqueous extract administration on (A): Gamma**
 394 **glutamyl transferase (GGT). (B): Butyrylcholinesterase (BChE).**

395 **3.8. Efficacy of saffron extract on myelin basic protein and acetylcholinesterase in the hippocampus**

396 The results in **Figure 10 (a and b)** revealed that levels of myelin Basic Protein (MBP), and
 397 acetylcholinesterase (AChE) were considerably higher in the induced group compared to the sham group.
 398 Concurrently, the co-administration of saffron extract (20,40&80mg/kg) notably reduced GFAP by
 399 (77.32%,88.37%&92.57%), MBP by (81.48%,85.60%&93.08%) and AChE by (46.15%,59.23%&74.41%) in all
 400 treated groups compared to the induced group. In addition, saffron80 returned MBP and AChE to the normal
 401 range.

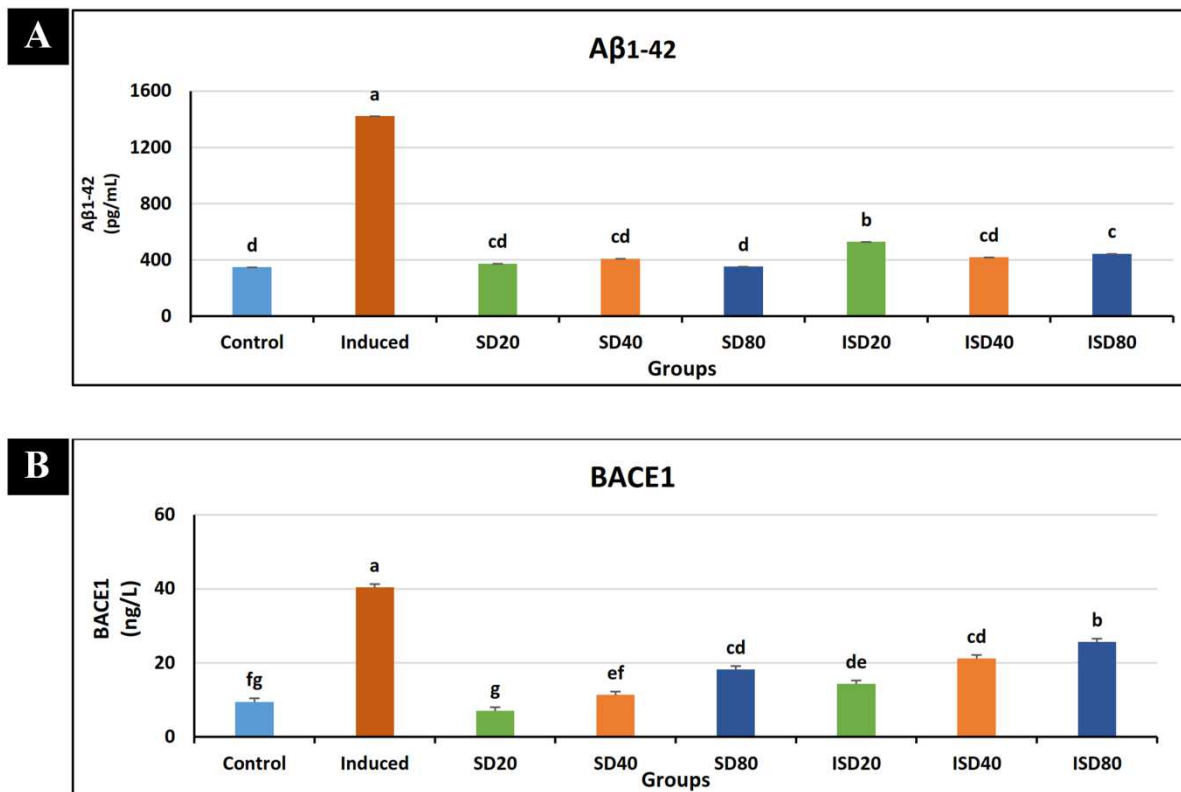


402

403 **Figure 10: (A and B):** Myelin Basic Protein (MBP) and Acetylcholinesterase (AChE) levels in
 404 hippocampus tissue homogenate.

405 **3.9. Attenuating effects of saffron crude extract supplementation on Alzheimer induced amyloid β -Peptide
 406 (1-42) ($A\beta$) plaque accumulation and beta-site amyloid precursor protein cleaving enzyme 1**

407 **Figure 11 (a and b)** displays the levels of beta-site amyloid precursor protein cleaving enzyme-1
 408 (BACE1) and amyloid β -Peptide (1-42) ($A\beta$ 1-42) in the hippocampal tissue homogenate. The findings
 409 demonstrated a substantial rise in BACE1 and $A\beta$ 1-42 levels in the STZ-induced group compared to the control
 410 group. Concurrently administering different dosages of SCE (20,40&80 mg/kg) resulted in a substantial decrease
 411 (BACE1) by (64.67%,47.59%&36.63%) and ($A\beta$ 1-42) by (62.94%,70.68%&68.925) in all treatment groups
 412 compared to induced group.



413
414

415 **Figure 11: (A and B)** Amyloid β -Peptide (1-42) (A β) plaque accumulation and beta-site
416 amyloid precursor protein cleaving enzyme 1(BACE1) levels in hippocampus tissue
417 homogenate

418 **3.10. Effects of saffron extract administration on pro-inflammatory and apoptotic biomarkers**

419 The findings in **Table (4)** showed an alarming increase in tumor necrosis factor-alpha (TNF- α),
420 interleukin 6 (IL-6), cyclooxygenase- 2 (COX-2), and cysteine-aspartic acid protease (Caspase-3) in the
421 stimulated group compared to the control group. Concurrently, supplementing saffron crude extract
422 (20,40&80mg/kg) notably reduced levels of TNF- α by (16.11%,32.04&55.63%), IL-6 by
423 (64.37%,64.37&89.84%), COX-2 by (82.58%,84.61&94.92%), and Caspase-3 by (14.42%,22.07&32.44%) in
424 all treated groups compared to the induced group. Moreover saffron 80 returned TNF- α , IL-6 and COX-2 to their
425 normal range.

426 **Table (4): Pro-fibrotic and oxidative stress biomarkers**

Parameter	Control	Induced	SD20	SD40	SD80	ISD20	ISD40	ISD80
TNF- α	103 ^c ± 15.43	339 ^a ± 8.82	124 ^c ± 11.48	102.6 ^c ± 12	116.2 ^c ± 16.62	284.4 ^b ± 1.63	230.4 ^b ± 11.99	150.4 ^c ± 10.72
IL-6	592 ^c ± 28.53	5984 ^a ± 149.18	489.6 ^c ± 21.73	577 ^c ± 14.8	628 ^c ± 14.63	2132 ^b ± 39.29	2132 ^b ± 39.30	607.60 ^c ± 30.43
COX-2	31.11 ^c ± 2.05	664 ^a ± 7.78	32.56 ^c ± 6.80	33.11 ^c ± 3.03	32.56 ^c ± 5.57	115.7 ^b ± 1.65	102.2 ^b ± 2.25	33.78 ^c ± 3.81
Caspase-3	6.618 ^e ± 0.081	10.77 ^a ± 0.151	6.68 ^e ± 0.36	6.67 ^e ± 0.045	6.63 ^e ± 0.118	9.23 ^b ± 0.029	8.39 ^c ± 0.069	7.27 ^d ± 0.185

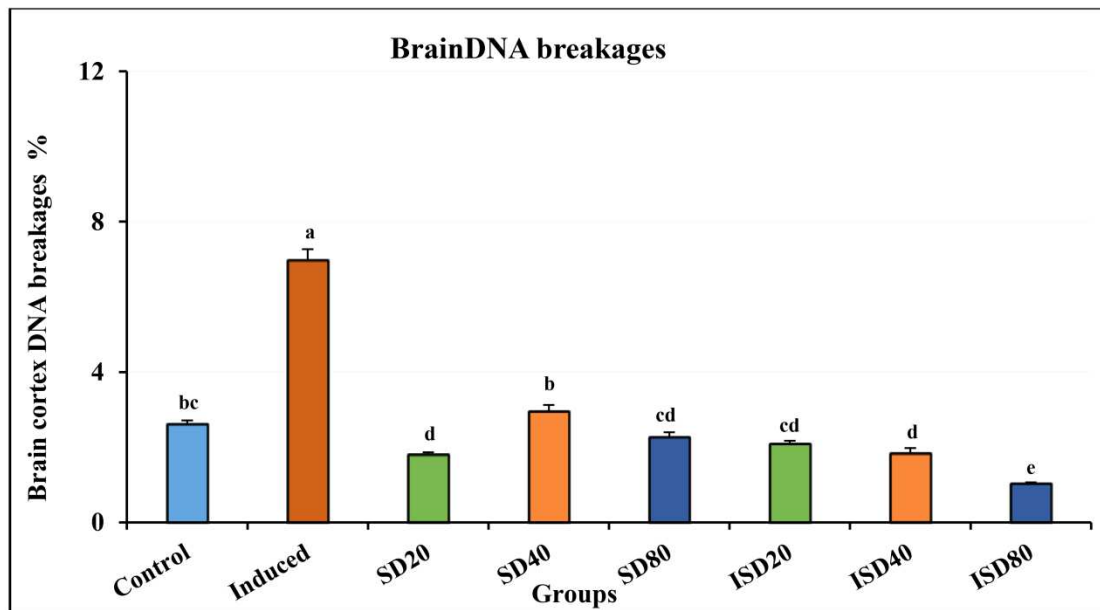
427 Tumor necrosis factor-alpha (TNF- α), interleukin 6 (IL-6), cyclooxygenase- 2 (COX-2), and cysteine-aspartic
428 acid protease (Caspase-3).

429 The results expressed as (Mean \pm SE, n=5)

430 ^{abcd} Mean values within columns not sharing common superscript letters were significantly different, p < 0.05.
431 control: sham group (citrate buffer), induced: STZ (3 mg/kg), SD20: saffron extract (20mg/kg), SD40: saffron
432 extract (40mg/kg), SD80: saffron extract (80mg/kg), ISD20: induced + saffron extract (20 mg/kg), ISD40:
433 induced + saffron extract (40 mg/kg) and ISD80: induced + saffron (80 mg/kg).

434 **3.11. Attenuating effect of saffron aqueous extract administration on DNA breakages in brain homogenate**

435 The results summarized in **Figure 12** indicate that the proportion of DNA breakage in the brain
436 significantly increased in the induced group compared to the control group. The administration of saffron crude
437 aqueous extract at varying doses (20, 40, and 80 mg/Kg) significantly reduced the percentage of DNA breakage
438 by (70.05%,73.63%&85.24%) compared to the stimulated group.



440 **Figure 12: Attenuating effect of saffron aqueous extract administration on DNA**
441 breakages in brain homogenate

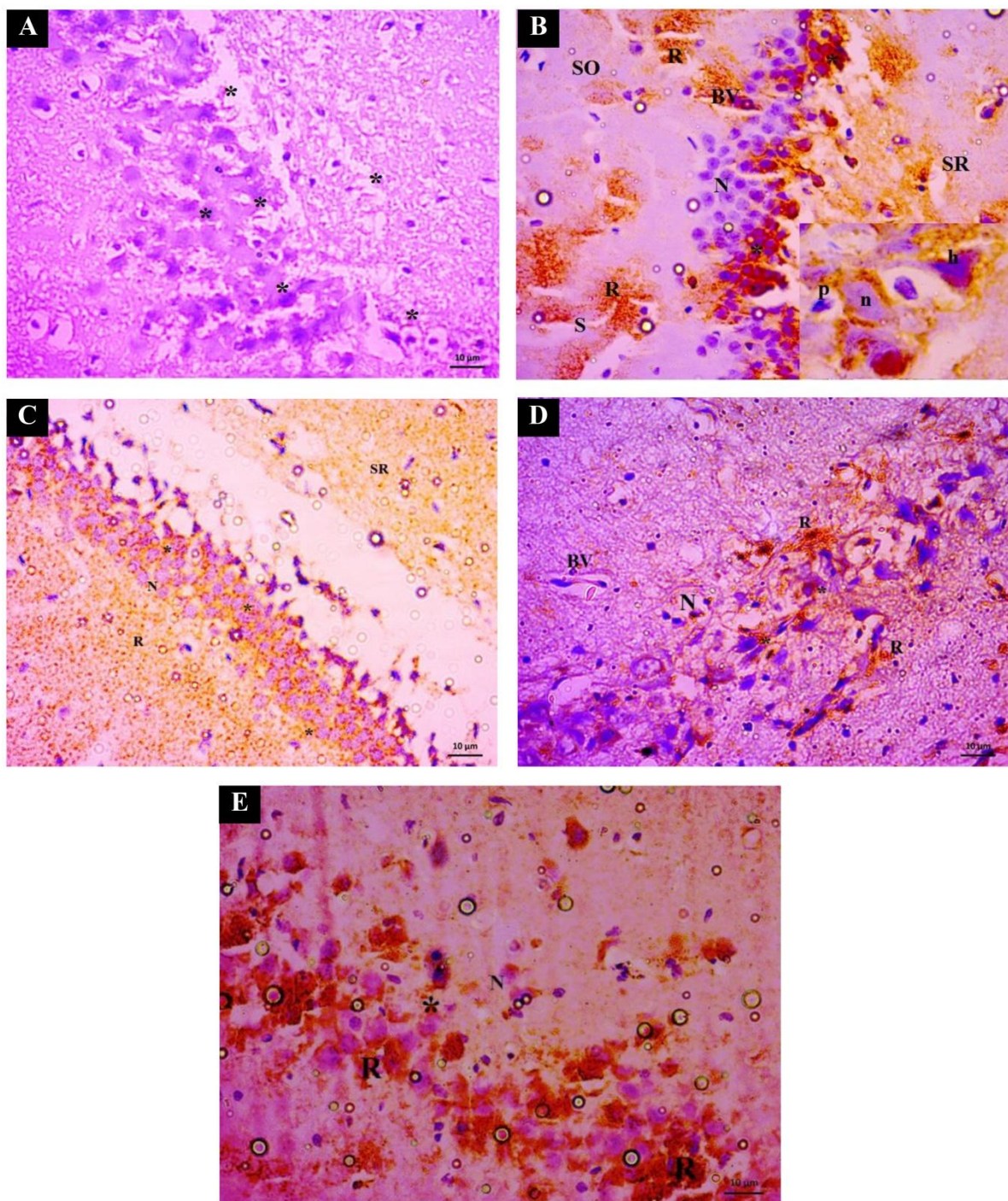
443

444 **3.12. Immunohistochemical Findings**

445 **a- Amyloid β (A β) peptide plaques**

446 Photomicrograph of a **control** rat brain subjected to treatment with ant. β -amyloid protein exhibits
447 negative immunostaining in the majority of neuropile cells inside the hippocampal area. The administration of
448 saffron extract was evaluated for its impact on amyloid plaque deposition in STZ-treated groups. Subsequently,
449 the photomicrograph of the **induced** rat brain exhibits robust immunostaining in the majority of neuropil cells
450 inside the hippocampal area. Endothelial blood vessels exhibited coarse, red-colored granules in the cytoplasm
451 and cell membrane, accompanied with a negative blue hue in the cell nucleus at CA3 demonstrates significant
452 immunostaining density within the hippocampal region in both stratum oriens (So) and stratum radiatum (Sr),
453 manifesting as a mass of red granular structures (R) encircling the dilated myelinated sheaths (S) and blood
454 vessels (BV). Numerous degenerative small and hyperchromatic pyramidal cells are evident as dark red
455 immunostaining in the cytoplasm, with thick, voluminous axons predominantly located in the upper regions of
456 the nuclei (*), alongside a negative blue hue in the neuronal cell nuclei (N). Most degenerative small and
457 hyperchromatic pyramidal cells are evident as dark red immunostaining in the cytoplasm, with thick, voluminous
458 axons predominantly located in the upper region of the nuclei (*), while the neuronal cell nuclei (N) exhibit a
459 negative blue coloration. In the box, an Alzheimer patch of the aggregated pyramidal cells exhibits a dense
460 coloration of beta-amyloid in the cytoplasm above the nuclei of necrotic (n), pyknotic (p), and hyperchromatic
461 (h) cells

462 Photomicrographs of the **ISD20** rat brain revealed a moderate reduction in immunostaining across the
463 majority of neuropil cells in the hippocampal regions So and Sr, presenting as a uniform yellowish hue.
464 Alterations in the neuronal tissue resulting from the administration of extract in the **ISD40** group rat brain
465 photomicrograph demonstrate a significant reduction in immunostaining in the majority of neuropile cells inside
466 the hippocampal regions So and Sr. Finally, a rat in group **ISD80**, exhibiting robust immunostaining in the
467 majority of neuropile cells inside the So and Sr regions of the hippocampus. The robust immunostaining in the
468 CA3 area neuron cells manifested as clusters of red granules in degenerative pyramidal cells, accompanied by a
469 negative blue hue in the nuclei as shown in **Figure 13 (a, b, c, d and e, respectively)**.



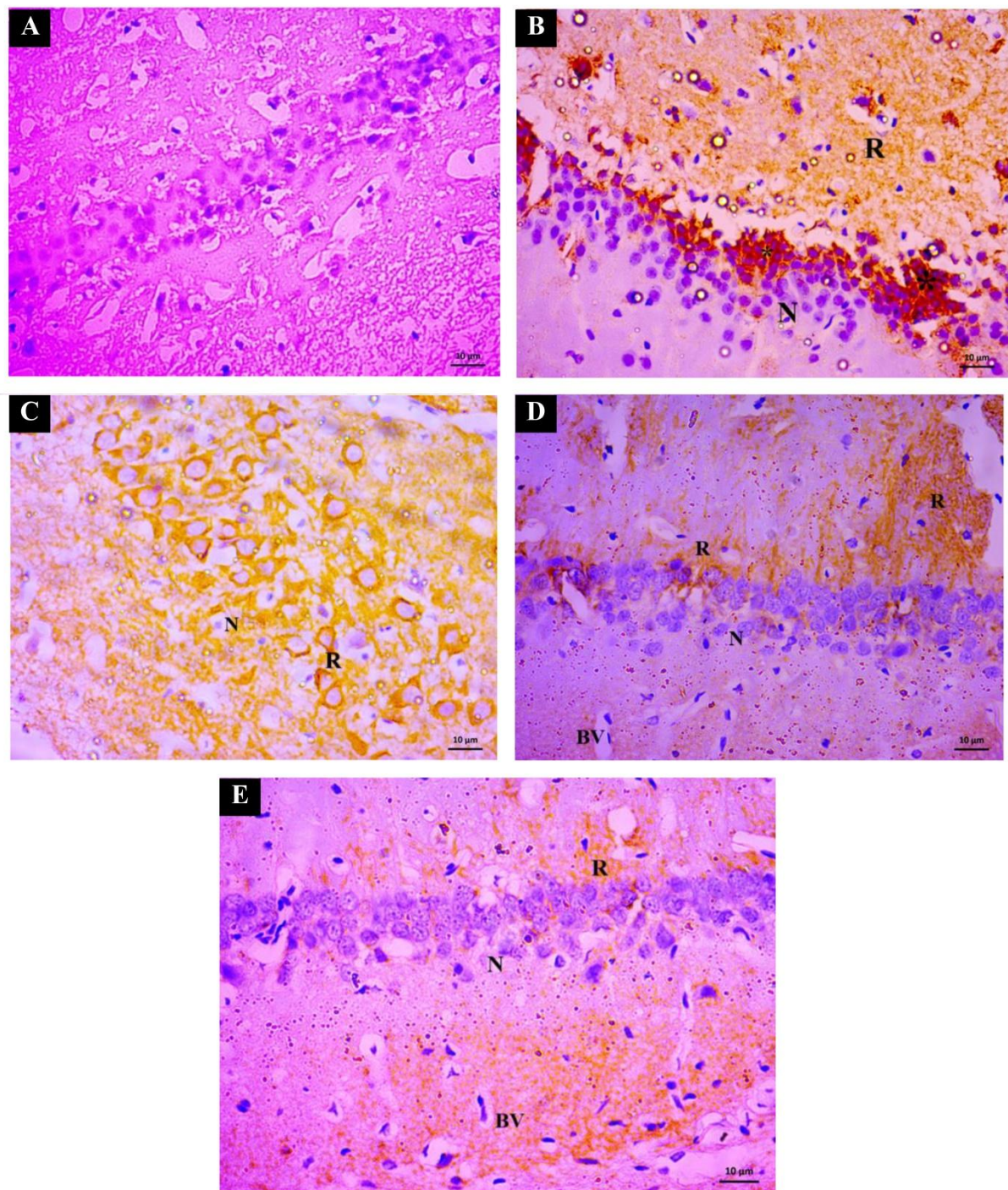
470
471

472 **Figure 13:** (A, B, C, D and E) Photomicrograph rat brain (A): control group, (B):
473 Induced group, (C): ISD20: induced + saffron extract (20 mg/kg), (D):
474 ISD40: induced + saffron extract (40 mg/kg) and (E): ISD80: induced +
475 saffron (80 mg/kg) treated by ant β -amyloid protein and stained by ACU, (β -
476 Am & ACU stain Bar=50 μ m)
477
478
479

480 **b- Tubulin associated unit (Tau)**

481 To investigate the effect of saffron extract on Alzheimer's disease, immunostaining of Tau protein in the
482 **control** group photomicrograph (Tau & ACU stain Bar=50 μ m) of the rat brain hippocampus demonstrates
483 negative immunostaining in the majority of neuropile cells within the hippocampal region. Alterations in
484 neuronal tissue resulting from the administration of streptozotocin to the induced group a photomicrograph
485 revealed pronounced immunostaining in the majority of neuropile cells within the hippocampal region,
486 manifesting as coarse red granules in the cytoplasm and diffuse filamentous deposition of staining in the stratum
487 region, accompanied by a negative blue coloration of the cell nuclei. Furthermore, at CA3, revealing pronounced
488 immunostaining density in the hippocampal region, manifested as red granular aggregates in the cytoplasm of
489 clustered astrocytes adjacent to degenerative, hyperchromatic pyramidal cells, along with diffuse
490 immunostaining in the cytoplasm of cells and small filaments of neural cells within the stratum region. A
491 negative blue hue of the neuronal cell nuclei (N)

492 Regarding the potential therapeutic efficacy of saffron extract on tau protein in the **ISD20 ,ISD40**, and
493 **ISD80** rat brain, moderate immunostaining was observed in the majority of neuropile cells within the
494 hippocampal region, manifesting as coarse red granules in the cytoplasm and diffuse filamentous deposition in
495 the stratum region, along with a limited presence of astrocytes in the DG region. Weak immunostaining of fine
496 filament deposition in the stratum region of select astrocytes in the dentate gyrus **Figure 14 (a,b,c,d and e)**
497 respectively.



498

499 **Figure 14:** (A, B, C, D and E) Photomicrograph rat brain (A): control group, (B): Induced
500 group, (C): ISD20: induced + saffron extract (20 mg/kg), (D): ISD40: induced
501 + saffron extract (40 mg/kg) and (E): ISD80: induced + saffron (80 mg/kg)
502 treated by tau protein and stained by ACU, (Tau & ACU stain Bar=50μm)

503

504

505

506 **4. Discussion**

507 To put things into perspective, Alzheimer's disease (AD) is the most common neurodegenerative cause of
508 dementia. Neurodegeneration is associated with toxic amyloid-beta (A β 1-42) oligomers and protein aggregates,
509 intra-neuronal neurofibrillary tangles consisting of hyperphosphorylated microtubule-associated Tau protein,
510 regionally specific reduction of cerebral glucose metabolism, synaptic dysfunction, and mitochondrial
511 dysfunction [33]. Prior research has demonstrated that administering low dosages of STZ directly into the brain
512 through the ICV route disrupts brain homeostasis, insulin signalling and impair in cerebral glucose metabolism.
513 This is characterized by neuropathological and metabolic alterations that resemble those seen in the
514 pathophysiology of AD, including synapse dysfunction, tau hyperphosphorylation, and oxidative stress [34].

515 In our study, the induction of AD was evident by behavioural and biochemical studies. To assess the effect
516 of SCE on cognitive impairment, the current study has shown that supplementation with aqueous extract of
517 saffron effectively counteracted Alzheimer-induced memory impairment at all supplemented dose levels.
518 Significant differences were observed in spatial and recognition memory in MWM and novel object recognition
519 assessments between the induced group and SCE-supplemented groups.

520 In the ORAC assessment, the reduction of indicator fluorescence displays a lag phase, wherein the
521 kinetics are defined by the rivalry between the interaction of peroxy radicals with the indicator and the
522 antioxidant [35]. The lag phase is analogous to that observed for oxygen intake during the suppression of
523 autoxidation by chain-breaking antioxidants and contrasts with competitive tests, such as crocin bleaching. The
524 ORAC assay evaluates an antioxidant's effectiveness by analysing the area under the curve of fluorescence
525 intensity over time, allowing for the assessment of peroxy radical reactions with a specific compound and the
526 determination of the total antioxidant capacity of a food extract. The ORAC assay presents potential benefits
527 over other methods by employing peroxy radicals as reactants with similar redox potential and reaction
528 mechanisms (i.e., hydrogen atom versus electron transfer) to physiological oxidants, and by utilizing a
529 physiological pH, enabling antioxidants to react under conditions that reflect the body's overall charge and
530 protonation state. The results derived from individual compounds demonstrate a correlation between the
531 fluorescence bleaching curve in the ORAC and the oxidation potential of the antioxidant. These findings are
532 anticipated to be widely useful for evaluating the total oxidation potential of more intricate combinations of
533 antioxidants, such as those present in food or plant extracts [31].

534 The Acetylcholinesterase inhibitory activity of saffron extract and its compounds derived from the
535 stigmas of *Crocus sativus* was assessed in a study to evaluate its potential application in combating Alzheimer's
536 disease. The experiment revealed Acetylcholinesterase inhibitory action in the saffron extract. The IC₅₀ values
537 of safranal, crocetin, and dimethyl crocetin were determined to be within the low micromolar range. A distinct
538 investigation utilized *Iris germanica* var. *Florentina* for the extraction of phenolic and flavonoid compounds.
539 Isolated fractions demonstrated suppression of both AChE and BChE, suggesting their possible application in
540 Alzheimer's disease treatment [36].

541 Our results show that untreated ICV-STZ-injected rats were impaired in the memory recall testing day as
542 they had a significantly lower preference for the target quadrant that had previously contained the platform.
543 Memory impairments in the MWM are among the major behavioural tests of rodent models of AD. This task is a
544 specific for model of AD because it taps hippocampal functions as it requires storing precise representation of
545 spatial relationships to locate a small, hidden goal. Significant differences in escape latency were observed in
546 acquisition and reference memory and novel object recognition assessments between the induced group and
547 SCE-supplemented groups. The percentage of time spent in the target quadrant and the travelled distance to
548 reach the hidden platform in each group were used to assess acquisition of the water maze task. The results
549 showed that in comparison with the control group, the ICV-STZ-injected rats revealed significant decline in
550 spatial learning, with longer latency and distance in reaching the hidden platform. Moreover, during the memory
551 retention test, rats failed to remember the precise location of the platform, spending significantly less time in the
552 target quadrant than the normal groups. Also, STZ rats failed to discriminate novel and familiar objects in object
553 recognition task. On the other hand, supplementation of SCE greatly enhanced the spatial and recognition
554 memory in both MWM and NOR tests. Saffron extract was also reported to have a positive impact on spatial
555 learning memory in morphine-induced memory impairment [37].

556 The anti-oxidative stress properties of saffron and crocin indicate a potential strategy for preventing
557 stress-induced damage to learning and memory. Saffron possesses have been attributed to many carotenoids that
558 have potent antioxidant properties and have the potential to safeguard central nervous system neurons from a
559 detrimental effect of oxidative stress [38].

560 In the hippocampal tissue homogenate, the level AChE were higher in the group treated for Alzheimer's
561 disease compared to the control group. However, after administering different dosages of SCE, AChE
562 dramatically decreased in all treated groups.

563 Acetylcholine, a neurotransmitter, enhances the propagation of nerve impulses and the conveyance of
564 signals related to memory and cognitive abilities. Increased AChE activity can lead to acetylcholine deficiency,
565 resulting in cholinergic dysfunction and cognitive impairments [39-41]. The cholinergic system is crucial for
566 attention, learning, and memory. It promotes nerve conduction and signal transduction related to memory and
567 learning ability [42]. However, the deterioration of cholinergic neuronal function leads to the accumulation of
568 AChE [43], tau phosphorylation, A β plaques, neurotoxicity, neuroinflammation, and neuronal death [44] which
569 ultimately results in condition like Alzheimer or dementia.

570 The result of the current study is consistent with previous finding where active constituent crocin also
571 increases acetylcholine levels which in turn decrease AChE, prevent hippocampal neuronal apoptosis, and
572 improve memory in the rat brain affected by Alzheimer [45]. Further, the molecular docking of extract
573 constituent at the active site of AChE also indicates that SCE constituents effectively inhibit the enzyme and
574 could increase the level of acetylcholine in the brain to improve memory [46].

575 In our study, we investigate the enzymes in blood serum associated with acetylcholinesterase function and
576 the impact of saffron extract on these enzymes. We assess the levels of gamma-glutamyl transferase (GGT),
577 which were significantly elevated in the induced group, while butyrylcholinesterase (BChE) was significantly
578 reduced in the induced group compared to the control group. Simultaneously, the co-administration of saffron
579 aqueous extract countered this effect in all treatment groups.

580 Gamma glutamyl transfers (GGT) has demonstrated a neuroprotective impact on neuronal cells. The
581 primary limitation of the vascular endothelial barrier is its failure to obstruct the ingress of lipophilic xenobiotics,
582 whereas Intracellular glutathione production, facilitated by GGT, can detoxify these compounds. Consequently,
583 GGT is pivotal in protecting cells from oxidative damage. Furthermore, elevated GGT levels within the normal
584 range may signify enhanced hepatic capacity to manage oxidative stress. A reduction in oxidative stress levels in
585 the body correlates the deficiency or lack of GGT results in a compromised glutamate cycle, adversely affecting
586 the absorption, transport, and use of amino acids, leading to disorders in glutathione resynthesis and increasing
587 neurological symptoms [47]. Therefore, a better GGT reserve is essential for generating enough glutathione to
588 maintain the redox balance in the body.

589 Primarily, to examine the impact of butyrylcholinesterase (BChE) on Alzheimer's disease, it is essential to
590 note that BChE hydrolyses acetylcholine (ACh). As BChE is an α -glycoprotein located in the central and
591 peripheral nervous systems, exhibiting a half-life of 12 days. It is a nonspecific or pseudocholinesterase, also
592 known as serum cholinesterase, which hydrolyses both choline and aliphatic esters [48].

593 The intracerebral infusion of STZ is known to cause memory impairment that closely resembles the
594 cognitive decline observed in sporadic Alzheimer's disease. Streptozotocin injected rats are used as a non-
595 transgenic rodent model to mimic Alzheimer's disease [49]. In this current investigation, thirty days following a
596 single ICV injection of STZ, the level of phosphorylated tau-217 significantly increased in STZ treated rats as
597 blood serum biomarkers that accurately indicate Alzheimer's disease. Meanwhile, co-administration of SCE
598 significantly decreased p tau-217 in all treated groups. Serum measures of phosphorylated tau have high
599 diagnostic accuracy in differentiating AD from other neurodegenerative disorders in clinical studies, which are
600 validated by postmortem neuropathological studies [50]. Tau proteins constitute a group of brain-specific
601 structural proteins present in microtubules. Their hyperphosphorylation causes abnormal folding and
602 fragmentation, giving rise to toxic insoluble aggregates inside cells, which are known as NFTs [1].

603 Above all a significant increase was observed in A β 1-42, MBP and BACE1 in induced group when
604 compared with control group.

605 The extracellular fibrillar amyloid β (A β) peptide plaques represent classical pathological hallmarks of
606 Alzheimer's disease. A β plaques form due to changes in amyloid precursor protein [21] metabolism. The
607 cleavage of APP by α -secretase leads to the production of non-amyloidogenic A β fragments, while cleavage by
608 β -secretase results in the formation of neurotoxic amyloidogenic A β fragments. A β aggregation triggers the
609 NFTs, neuronal dysfunction, and dementia [51]. Furthermore, high level of AChE not only down regulates
610 acetylcholine function but also combines with A β fibrils and forms more neurotoxic AChE-A β complex which
611 further exaggerate neurodegeneration than those of A β fibrils alone [52].

612 The β -cleaving secretase, BACE1, define a family of transmembrane aspartic proteases [53]. BACE1
613 exhibits all the properties of the β -secretase and is the key rate-limiting enzyme that initiates the formation of A β
614 [54]. BACE1 is principally present in neurons in the central nervous system [55]. Higher β -secretase activity, as
615 well as induction of BACE1 protein level, is seen in AD brains. Another interesting observation is that induced
616 BACE1 protein appears to colocalize with markers of apoptosis. This is consistent with the role of apoptosis in
617 AD. In neurodegenerative diseases including AD, signals that initiate neuronal apoptosis, including neurotrophic
618 factor support withdraw, disturbance of calcium homeostasis, increased oxidative stress and metabolic stress, are
619 described [56]. These pro-apoptotic factors may contribute to the over-expression of BACE protein in the AD
620 brain, and interfere with APP processing, thus seeding formation of senile plaques. This BACE activation can
621 then cause further apoptotic signalling, inducing caspase activation and DNA fragmentation, both of which are
622 observed in AD brains [57].

623 The current study indicate that induction of AD with STZ significantly increase MBP which is one of the
624 most abundant proteins in the myelin sheath and the only structural myelin protein known to be essential for the
625 formation of compact myelin sheaths as well as it is a multifunctional protein that interacts with lipids and a
626 diverse array of proteins [58].Concurrently, the co-administration of SCE resulted in a significant drop in MBP
627 across all dosages. However, in the case of saffron 80, MBP restored to its usual range. Specifically, MBP
628 regulates voltage-gated Ca $^{2+}$ channels (VGCCs) at the plasma membrane reducing the Ca $^{2+}$ influx in the
629 oligodendrocyte. Numerous studies have indicated that the absence of this protein leads to myelin vesiculation
630 and subsequent breakdown. However, there is no study describing the opposite effect. It is therefore plausible
631 that an excess accumulation of this protein might influence myelin compaction, subsequently affecting
632 conduction velocity and the delivery of nutrients to the axon [59].

633 Upregulation of MBP inhibits VGCCs, thereby reducing Ca $^{2+}$ influx into oligodendrocytes. Ca $^{2+}$ influx
634 through membrane channels is a critical step in signalling pathways involved in the regulation of growth,
635 maturation and functional plasticity. In addition, elevated Ca $^{2+}$ levels stimulate MBP synthesis in
636 oligodendrocytes [60] and are critical for myelin sheath extension. The accumulation of MBP in the membrane
637 would inhibit or reduce the number of VGCCs in the membrane, as previously reported [61], thereby affecting to
638 the calcium entry through these channels. Thus, our results suggest that A β oligomers disrupt Ca $^{2+}$ regulation,
639 making oligodendrocytes more susceptible to environmental stimuli that increase intracellular Ca $^{2+}$ levels and
640 affect myelination.

641 Increased levels of MBP protein in AD cortex have been reported in at least one previous study [62].
642 Thus, our results confirm that the levels of MBP and degraded myelin basic protein complex (dMBP) are
643 increased in AD cortex compared to controls. The mechanism by which that MBP levels were higher in AD
644 compared to control remains unclear. It is possible that MBP/myelin injury is associated with remyelination
645 which increases total MBP in AD brain. In addition, we cannot rule out the possibility that the increase in
646 "MBP" observed in AD brain is due to induction of Golli MBP proteins that are normally expressed in neurons
647 [63].

648 Investigations show a close link between BChE and A β , the major pathogenic feature of Alzheimer's
649 disease. According to the A β hypothesis, β - and γ -secretases successively digest amyloid precursor protein,
650 producing damaging full-length A β 1-40/42 peptides. In Alzheimer's disease patients, an imbalance between A β
651 production and clearance in the nervous system leads to irreversible accumulation of A β plaques and
652 pathological processes. Microglia play a crucial role in clearing extraneuronal A β plaques [64]. Based on the
653 aforementioned evidence, inhibiting BChE instead of AChE may represent a more promising and effective
654 therapeutic approach for patients with advanced Alzheimer's disease, without inducing significant side effects.

655 In the present study potential of saffron crude extract (SCE) to reduce neurodegeneration dysfunction
656 induced cholinergic disturbance and associated changes caused by STZ were investigated. Further, the impact of
657 SCE on AChE, and proinflammatory cytokine i.e., IL-6, COX-2, Caspase-3 and TNF- α were explored.

658 The brain's cellular membrane is rich in polyunsaturated fatty acids (PUFA), making it more vulnerable to
659 neuroinflammation [65], which in turn lead amyloid and tau pathologies [66]. Streptozotocin administration
660 releases of pro-inflammatory cytokines and accelerates neurodegeneration [67]. In this study, STZ significantly
661 elevated IL-6, COX-2, Caspase 3 and TNF- α which was countered by SCE supplementation which significantly
662 decreases in all dose levels. This is also supported by previous literature in which saffron extract and crocin has
663 shown a neuroprotective role against methamphetamine neurotoxicity in rats by arresting proinflammatory
664 cytokines production [68].

665 Oxidative stress is increasingly thought to be involved in various neurodegenerative diseases. Elevated
666 oxidative damage was identified as a common characteristic in neurons and peripheral cells from both sporadic
667 and familial Alzheimer's disease patients. Data suggests that oxidative stress manifests early in Alzheimer's
668 disease, somewhat prior to the emergence of pathological markers such as neurofibrillary tangles and senile
669 plaques [69]. The deposition of insoluble A β forms is considered a cause of oxidative stress in Alzheimer's
670 disease, with A β hypothesized as the originator of this process. The accumulation of hyperphosphorylated tau,
671 synaptic loss, and axonal degeneration are pathogenic characteristics of Alzheimer's disease. Tau not only
672 stabilizes microtubules and promotes neurite development but also regulates the movement of cellular
673 components via molecular motors along microtubules. Misregulation of tau protein leads to the progressive
674 retraction of cellular organelles, including mitochondria and peroxisomes, resulting in synaptic starvation and
675 heightened oxidative stress due to the lack of catalase in peroxisomes [70]. It has been noted that A β deposition
676 occurs subsequent to elevated levels of 8-Hydroxy-2-deoxyguanosine (8-OHdG), and that 8-OHdG levels return
677 to baseline following the formation of A β plaques. Oxidative damage refers to the formation of reactive oxygen
678 species (ROS), which can alter the structure of proteins, lipids, and nucleic acids through interaction. The comet
679 assay, a novel methodology for evaluating DNA damage, is an effective test for genotoxicity and serves as a
680 crucial instrument for exploring fundamental elements of DNA damage and subsequent cellular responses [71].

681 Saffron and its constituents can safeguard DNA and RNA from destructive chemical reactions [72]. The
682 constituents of saffron demonstrate potential antioxidant properties, allowing free radicals to withdraw a
683 hydrogen atom from the antioxidant molecule rather than from polyunsaturated fatty acids (PUFA), thus
684 disrupting the sequence of free radical reactions, resulting in an antioxidant radical that is a relatively
685 nonreactive entity [73] both ethanolic and aqueous extracts of saffron have been shown to possess antioxidant
686 activity through various in vitro methods, specifically employing three experimental approaches: the deoxyribose
687 assay, erythrocyte membrane peroxidation, and rat liver microsomal lipid peroxidation induced by
688 Fe $^{2+}$ /ascorbate. Crocin, a primary carotenoid in saffron, has exhibited supplementary roles concerning the
689 antioxidant properties of saffron. Safranal, a monoterpenal aldehyde and the primary constituent of saffron's
690 essential oil, also exhibits antioxidant properties.

691 Multiple investigations have demonstrated that the active compound of *Crocus sativus* reduces A β fibril
692 production and neuronal apoptosis [74], alters the A β aggregation pathway, and forms stable fibrils by changing
693 the distribution of A β 1-40 [75]. Crocin lowers A β , and p-tau levels via altering MAPK signalling pathways [76]
694 and enhancing the expression of A β -degrading enzymes. The acetylcholinesterase inhibitory action of CSE
695 components in the active site of the galantamine binding receptor resembles that of conventional medications
696 rivastigmine and galantamine. These results come in align with our results.

697 Conclusion

698 To summarize, this study shows that the standardized aqueous SCE has the ability to inhibit the activity of
699 acetylcholinesterase and operate as an antioxidant. Additionally, it has been found to reduce the negative effects
700 on learning and memory caused by Alzheimer. Administration of SCE effectively reduces the occurrence of A β
701 plaque and the level of phosphorylated tau-217 and MBP in the hippocampus at various dosage levels.
702 Furthermore, SCE also mitigates the inflammation caused by Alzheimer disease. The findings suggest that a
703 botanical supplement derived from Saffron may have potential in the treatment of senile dementia.

704
705
706
707
708
709
710
711
712

713 **References:**

714 1. Yu, X., Li Y. & Mu X. Effect of Quercetin on PC12 Alzheimer's Disease Cell Model Induced by A β 25-
715 35 and Its Mechanism Based on Sirtuin1/Nrf2/HO-1 Pathway. *BioMed Res. Int.* **2020**, 8210578 (2020).

716 2. Andrade-Guerrero, J., *et al.* Alzheimer's Disease: An Updated Overview of Its Genetics. *Int. J. Mol. Sci.*
717 **24**, 3754 (2023).

718 3. Knopman, D. S., *et al.* Alzheimer disease. *Nat. Rev. Dis. Primers.* **7**, 33 (2021).

719 4. Hernández-Rodríguez, M., *et al.* Contribution of hyperglycemia-induced changes in microglia to
720 Alzheimer's disease pathology. *Pharmacol Rep.* **74**, 832-846 (2022).

721 5. Kepp, K. P., Robakis N. K., Høilund-Carlsen P. F., Sensi S. L. & Vissel B. The amyloid cascade
722 hypothesis: an updated critical review. *Brain.* **146**, 3969-3990 (2023).

723 6. Boggs, J. M. Myelin basic protein: a multifunctional protein. *Cell Mol. Life Sci.* **63**, 1945-1961 (2006).

724 7. Teunissen, C. E., Thijssen E. H. & Verberk I. M. W. Plasma p-tau217: from 'new kid' to most promising
725 candidate for Alzheimer's disease blood test. *Brain.* **143**, 3170-3172 (2020).

726 8. Ashton, N. J., *et al.* A multicentre validation study of the diagnostic value of plasma neurofilament light.
727 *Nat. Commun.* **12**, 3400 (2021).

728 9. Montoliu-Gaya, L., *et al.* Mass spectrometric simultaneous quantification of tau species in plasma shows
729 differential associations with amyloid and tau pathologies. *Nat. Aging.* **3**, 661-669 (2023).

730 10. Jonaitis, E. M., *et al.* Plasma phosphorylated tau 217 in preclinical Alzheimer's disease. *Brain Commun.*
731 **5**, fcad057 (2023).

732 11. Bhat, B. A., *et al.* Natural Therapeutics in Aid of Treating Alzheimer's Disease: A Green Gateway Toward
733 Ending Quest for Treating Neurological Disorders. *Front. Neurosci.* **16**, 884345 (2022).

734 12. D'Onofrio, G., Nabavi S. M., Sancarlo D., Greco A. & Pieretti S. Crocus Sativus L. (Saffron) in
735 Alzheimer's Disease Treatment: Bioactive Effects on Cognitive Impairment. *Curr Neuropharmacol.* **19**,
736 1606-1616 (2021).

737 13. Farokhnia, M., *et al.* Comparing the efficacy and safety of Crocus sativus L. with memantine in patients
738 with moderate to severe Alzheimer's disease: a double-blind randomized clinical trial. *Hum
739 Psychopharmacol.* **29**, 351-359 (2014).

740 14. Tarantilis, P. A., Polissiou M. & Manfait M. Separation of picrocrocin, cis-trans-crocins and safranal of
741 saffron using high-performance liquid chromatography with photodiode-array detection. *J. Chromatogr.
742 A.* **664**, 55-61 (1994).

743 15. Apak, R., *et al.* Comparative Evaluation of Various Total Antioxidant Capacity Assays Applied to
744 Phenolic Compounds with the CUPRAC Assay. *Molecules.* **12**, 1496-1547 (2007).

745 16. Re, R., *et al.* Antioxidant activity applying an improved ABTS radical cation decolorization assay. *Free
746 Radic. Biol. Med.* **26**, 1231-1237 (1999).

747 17. Ou, B., Huang D., Hampsch-Woodill M., Flanagan J. A. & Deemer E. K. Analysis of antioxidant
748 activities of common vegetables employing oxygen radical absorbance capacity (ORAC) and ferric
749 reducing antioxidant power (FRAP) assays: a comparative study. *J. Agric. Food Chem.* **50**, 3122-3128
750 (2002).

751 18. Vinutha, B., *et al.* Screening of selected Indian medicinal plants for acetylcholinesterase inhibitory
752 activity. *J. Ethnopharmacol.* **109**, 359-363 (2007).

753 19. Kraska, A., *et al.* In vivo cross-sectional characterization of cerebral alterations induced by
754 intracerebroventricular administration of streptozotocin. *PLoS One.* **7**, e46196 (2012).

755 20. Farjah, G. H., Salehi S., Ansari M. H. & Pourheidar B. Protective effect of *Crocus sativus* L. (Saffron)
756 extract on spinal cord ischemia-reperfusion injury in rats. *Iran J. Basic Med. Sci.* **20**, 334-337 (2017).

757 21. Gruss, M., *et al.* 9-Methyl- β -carboline-induced cognitive enhancement is associated with elevated
758 hippocampal dopamine levels and dendritic and synaptic proliferation. *J. Neurochem.* **121**, 924-931
759 (2012).

760 22. BÜTtnér-Ennever, J. The Rat Brain in Stereotaxic Coordinates, 3rd edn. By George Paxinos and Charles
761 Watson. (Pp. xxxiii+80; illustrated; £\$69.95 paperback; ISBN 0 12 547623; comes with CD-ROM.) San
762 Diego: Academic Press. 1996. *J. Anat.* **191**, 315-317 (1997).

763 23. Morris, R. G. M., Garrud P., Rawlins J. N. P. & O'Keefe J. Place navigation impaired in rats with
764 hippocampal lesions. *Nature*. **297**, 681-683 (1982).

765 24. Terry Jr, A. V. Spatial navigational (water maze) tasks. In *Methods of behavior analysis in neuroscience*.
766 (ed. Buccafusco JJ) 169-182 (CRC Press, 2000).

767 25. Bevins, R. A. & Besheer J. Object recognition in rats and mice: a one-trial non-matching-to-sample
768 learning task to study 'recognition memory'. *Nat. Protoc.* **1**, 1306-1311 (2006).

769 26. Knedel, M. & Böttger R. A kinetic method for determination of the activity of pseudocholinesterase
770 (acylcholine acyl-hydrolase 3.1.1.8.). *Klin. Wochenschr.* **45**, 325-327 (1967).

771 27. Wu, B., *et al.* T Cell Deficiency Leads to Liver Carcinogenesis in Azoxymethane-Treated Rats. *Exp. Biol.*
772 *Med.* **231**, 91-98 (2006).

773 28. Bućan, M. & Abel T. The mouse: Genetics meets behaviour. *Nat. Rev. Genet.* **3**, 114-123 (2002).

774 29. George, D. & Mallory P. *IBM SPSS statistics 26 step by step: A simple guide and reference*. (Routledge,
775 2019).

776 30. Athmouni, K., Belghith T., Fek A. & Ayadi H. Phytochemical composition and antioxidant activity of
777 extracts of some medicinal plants in Tunisia. *Int. J. Pharmacol. Toxicol.* **4**, 159 (2016).

778 31. Bisby, R. H., Brooke R. & Navaratnam S. Effect of antioxidant oxidation potential in the oxygen radical
779 absorption capacity (ORAC) assay. *Food Chem.* **108**, 1002-1007 (2008).

780 32. Mukherjee, P. K., Kumar V., Mal M. & Houghton P. J. Acetylcholinesterase inhibitors from plants.
781 *Phytomedicine*. **14**, 289-300 (2007).

782 33. Legname, G. & Scialò C. On the role of the cellular prion protein in the uptake and signaling of
783 pathological aggregates in neurodegenerative diseases. *Prion*. **14**, 257-270 (2020).

784 34. Park, J., *et al.* Streptozotocin Induces Alzheimer's Disease-Like Pathology in Hippocampal Neuronal
785 Cells via CDK5/Drp1-Mediated Mitochondrial Fragmentation. *Front. Cell. Neurosci.* **14**, 235 (2020).

786 35. Huang, D., Ou B. & Prior R. L. The Chemistry behind Antioxidant Capacity Assays. *J. Agric. Food*
787 *Chem.* **53**, 1841-1856 (2005).

788 36. Ullah, F., *et al.* Phenolic, flavonoid contents, anticholinesterase and antioxidant evaluation of Iris
789 germanica var; florentina. *Nat. Prod. Res.* **30**, 1440-1444 (2016).

790 37. Kiashemshaki, B., Safakhah H.-A., Ghanbari A., Khaleghian A. & Miladi-Gorji H. Saffron (*Crocus*
791 *sativus* L.) stigma reduces symptoms of morphine-induced dependence and spontaneous withdrawal in
792 rats. *Am. J. Drug Alcohol Abuse*. **47**, 170-181 (2021).

793 38. Ochiai, T., *et al.* Protective effects of carotenoids from saffron on neuronal injury in vitro and in vivo.
794 *Biochim. Biophys. Acta*. **1770**, 578-584 (2007).

795 39. Pepeu, G., Giovannini M. G. & Bracco L. Effect of cholinesterase inhibitors on attention. *Chem. Biol.*
796 *Interact.* **203**, 361-364 (2013).

797 40. Singh, S. P. & Gupta D. Discovery of potential inhibitor against human acetylcholinesterase: a molecular
798 docking and molecular dynamics investigation. *Comput. Biol. Chem.* **68**, 224-230 (2017).

799 41. Maurer, S. V. & Williams C. L. The cholinergic system modulates memory and hippocampal plasticity via
800 its interactions with non-neuronal cells. *Front. Immunol.* **8**, 1489 (2017).

801 42. Picciotto, Marina R., Higley Michael J. & Mineur Yann S. Acetylcholine as a Neuromodulator:
802 Cholinergic Signaling Shapes Nervous System Function and Behavior. *Neuron.* **76**, 116-129 (2012).

803 43. Huang, Q., Liao C., Ge F., Ao J. & Liu T. Acetylcholine bidirectionally regulates learning and memory. *J.*
804 *Neurorestoratol.* **10**, 100002 (2022).

805 44. Majdi, A., *et al.* Amyloid- β , tau, and the cholinergic system in Alzheimer's disease: seeking direction in a
806 tangle of clues. *Rev. Neurosci.* **31**, 391-413 (2020).

807 45. Saeedi, M. & Rashidy-Pour A. Association between chronic stress and Alzheimer's disease: Therapeutic
808 effects of Saffron. *Biomed. Pharmacother.* **133**, 110995 (2021).

809 46. Walczak-Nowicka, L. J. & Herbet M. Acetylcholinesterase Inhibitors in the Treatment of
810 Neurodegenerative Diseases and the Role of Acetylcholinesterase in their Pathogenesis. *Int. J. Mol. Sci.*
811 **22**, 9290 (2021).

812 47. Ristoff, E. & Larsson A. Inborn errors in the metabolism of glutathione. *Orphanet J. Rare Dis.* **2**, 16
813 (2007).

814 48. Paes, A. M. A., Carniatto S. R., Francisco F. A., Brito N. A. & Mathias P. C. F. Acetylcholinesterase
815 Activity Changes on Visceral Organs of VMH Lesion-Induced Obese Rats. *Int. J. Neurosci.* **116**, 1295-
816 1302 (2006).

817 49. Chen, Y., *et al.* A Non-transgenic Mouse Model (icv-STZ Mouse) of Alzheimer's Disease: Similarities to
818 and Differences from the Transgenic Model (3xTg-AD Mouse). *Mol. Neurobiol.* **47**, 711-725 (2013).

819 50. Milà-Alomà, M., *et al.* Plasma p-tau231 and p-tau217 as state markers of amyloid- β pathology in
820 preclinical Alzheimer's disease. *Nat. Med.* **28**, 1797-1801 (2022).

821 51. d'Errico, P. & Meyer-Luehmann M. Mechanisms of pathogenic tau and A β protein spreading in
822 Alzheimer's disease. *Front. Aging Neurosci.* **12**, 265 (2020).

823 52. Talesa, V. N. Acetylcholinesterase in Alzheimer's disease. *Mech. Ageing Dev.* **122**, 1961-1969 (2001).

824 53. Vassar, R. β -Secretase (BACE) as a drug target for Alzheimer's disease. *Adv. Drug Deliv. Rev.* **54**, 1589-
825 1602 (2002).

826 54. Murphy, T., *et al.* The BACE gene: genomic structure and candidate gene study in late-onset Alzheimer's
827 disease. *NeuroReport.* **12**, 631-634 (2001).

828 55. Vassar, R., *et al.* Beta-secretase cleavage of Alzheimer's amyloid precursor protein by the transmembrane
829 aspartic protease BACE. *Science.* **286**, 735-741 (1999).

830 56. LaFerla, F. M. Calcium dysregulation and intracellular signalling in Alzheimer's disease. *Nat. Rev.*
831 *Neurosci.* **3**, 862-872 (2002).

832 57. Fukumoto, H., Cheung B. S., Hyman B. T. & Irizarry M. C. β -Secretase Protein and Activity Are
833 Increased in the Neocortex in Alzheimer Disease. *Arch. Neurol.* **59**, 1381-1389 (2002).

834 58. Harauz, G. & Boggs J. M. Myelin management by the 18.5-kDa and 21.5-kDa classic myelin basic
835 protein isoforms. *J. Neurochem.* **125**, 334-361 (2013).

836 59. Weil, M.-T., *et al.* Loss of myelin basic protein function triggers myelin breakdown in models of
837 demyelinating diseases. *Cell Rep.* **16**, 314-322 (2016).

838 60. Friess, M., *et al.* Intracellular ion signaling influences myelin basic protein synthesis in oligodendrocyte
839 precursor cells. *Cell Calcium.* **60**, 322-330 (2016).

840 61. Smith, G. S. T., *et al.* Classical 18.5-and 21.5-kDa isoforms of myelin basic protein inhibit calcium influx
841 into oligodendroglial cells, in contrast to golli isoforms. *J. Neurosci. Res.* **89**, 467-480 (2011).

842 62. Selkoe, D. J., Brown B. A., Salazar F. J. & Marchotta C. A. Myelin basic protein in Alzheimer disease
843 neuronal fractions and mammalian neurofilament preparations. *Ann. Neurol.* **10**, 429-436 (1981).

844 63. Zhan, X., *et al.* Myelin Basic Protein Associates with A β PP, A β 1-42, and Amyloid Plaques in Cortex of
845 Alzheimer's Disease Brain. *J. Alzheimers Dis.* **44**, 1213-1229 (2015).

846 64. Fang, E. F., *et al.* Mitophagy inhibits amyloid- β and tau pathology and reverses cognitive deficits in
847 models of Alzheimer's disease. *Nat. Neurosci.* **22**, 401-412 (2019).

848 65. Gómez-Ramos, A., Díaz-Nido J., Smith M. A., Perry G. & Avila J. Effect of the lipid peroxidation
849 product acrolein on tau phosphorylation in neural cells. *J. Neurosci. Res.* **71**, 863-870 (2003).

850 66. Liu, P., Wang Y., Sun Y. & Peng G. Neuroinflammation as a Potential Therapeutic Target in Alzheimer's
851 Disease. *Clin. Interv. Aging.* **17**, 665-674 (2022).

852 67. Cheon, S. Y., *et al.* Scopolamine promotes neuroinflammation and delirium-like neuropsychiatric disorder
853 in mice. *Sci. Rep.* **11**, 8376 (2021).

854 68. Shafahi, M., Vaezi G., Shajiee H., Sharafi S. & Khaksari M. Crocin Inhibits Apoptosis and Astrogliosis of
855 Hippocampus Neurons Against Methamphetamine Neurotoxicity via Antioxidant and Anti-inflammatory
856 Mechanisms. *Neurochem. Res.* **43**, 2252-2259 (2018).

857 69. Perry, G., *et al.* Is oxidative damage the fundamental pathogenic mechanism of Alzheimer's and other
858 neurodegenerative diseases? *Free Radic. Biol. Med.* **33**, 1475-1479 (2002).

859 70. Wu, M. F., Yin J. H., Hwang C. S., Tang C. M. & Yang D. I. NAD attenuates oxidative DNA damages
860 induced by amyloid beta-peptide in primary rat cortical neurons. *Free Radic. Re.* **48**, 794-805 (2014).

861 71. Blair, I. A. Lipid hydroperoxide-mediated DNA damage. *Exp. Gerontol.* **36**, 1473-1481 (2001).

862 72. Abdullaev, F. I., *et al.* Use of in vitro assays to assess the potential antigenotoxic and cytotoxic effects of
863 saffron (*Crocus sativus* L.). *Toxicol. In Vitro.* **17**, 731-736 (2003).

864 73. Hosseinzadeh, H., Shamsaie F. & Mehri S. Antioxidant activity of aqueous and ethanolic extracts of
865 *Crocus sativus* L. stigma and its bioactive constituents, crocin and safranal. *Pharmacogn. Mag.* **5**, 419-
866 424 (2009).

867 74. Ghahghaei, A., Bathaie S. Z. & Bahraminejad E. Mechanisms of the Effects of Crocin on Aggregation
868 and Deposition of A β 1-40 Fibrils in Alzheimer's Disease. *Int. J. Pept. Res. Ther.* **18**, 347-351 (2012).

869 75. Koulakiotis, N. S., Purhonen P., Gikas E., Hebert H. & Tsarbopoulos A. Crocus-derived compounds alter
870 the aggregation pathway of Alzheimer's Disease - associated beta amyloid protein. *Sci. Rep.* **10**, 18150
871 (2020).

872 76. Rashedinia, M., Lari P., Abnous K. & Hosseinzadeh H. Protective effect of crocin on acrolein-induced tau
873 phosphorylation in the rat brain. *Acta Neurobiol. Exp.* **75**, 208-219 (2015).

874
875

876 **Author contributions:**

877 Aly B. Okab: propose the research point, design the experiment and supervising the practical parts, supervising
878 the physiological studies; Sabah G. Elbanna: propose the research point, design the experiment and supervising
879 the practical parts, supervising the biochemical studies, and supervising analysis of results; Abeer Salama:
880 Contributing in methodology, Resources and statistical analysis ;Seham Z. Nassar: Shared in the
881 conceptualization of the study, stereotaxic technique for ICV injection and the behavioural studies conduction
882 and interpretation; Naglaa H. Eldewany: Propose the research point , conducted the experiments and the practical
883 part, interpretation of data, Statistical analysis and wrote the manuscript; Aly B. Okab, Sabah G. Elbanna, Abeer
884 Salama, Seham Z. Nassar and Naglaa H. Eldewany: All authors finally reviewed, editing and agreed with the
885 content of the manuscript.

886 **Data availability statement:**

887 Data will be made available on request.

888 **Approval of animal experiments:**

889 The experiments were approved by the Ethical Committee of the National Research Centre, Egypt, and
890 the Institutional Animal Care and Use Committee, Faculty of Medicine, Alexandria University (ALEXU-IACUC
891 No. AU14-231130-2-12), Alexandria, Egypt.

892 **Competing Interests Statement:**

893 The authors declare no competing interests.

894 **Funding:**

895 This research did not receive any specific grant from funding agencies in the public, commercial, or not-for-
896 profit sectors.

897 **Conflicts of Interest:**

898 The authors declare no conflict of interest pertaining to this research work.